On the Cover: Lymph node reticular cells provide survival factors for lymphocytes and can potentially be targeted in disease. However, the mechanisms that regulate reticular cell function during ongoing immune responses are not well understood. In this issue of Immunity, Kumar et al. (719–730) show that dendritic cells maintain podoplanin (PDPN)+ reticular cell survival in inflamed, but not homeostatic, lymph nodes. The cover image shows a PDPN+ reticular cell (the tree) that nourishes and supports lymphocytes (the birds) by expressing lymphocyte survival factors (the fruit). During an immune response (the storm), the reticular cell (the tree) requires the help of dendritic cells (the men on the ground) to survive. The dendritic cells express lymphotoxin-β receptor ligands (the hands of the men), which modulate PDPN (the ropes). PDPN signals to promote activity of β1 integrins (the tree roots). β1-integrin-mediated cell-matrix adhesion (the tree staying rooted) helps the reticular cell to survive and function. Illustration drawn by Dragos Dasoveanu with assistance by Varsha Kumar.

On the Cover: Lymph node reticular cells provide survival factors for lymphocytes and can potentially be targeted in disease. However, the mechanisms that regulate reticular cell function during ongoing immune responses are not well understood. In this issue of Immunity, Kumar et al. (719–730) show that dendritic cells maintain podoplanin (PDPN)+ reticular cell survival in inflamed, but not homeostatic, lymph nodes. The cover image shows a PDPN+ reticular cell (the tree) that nourishes and supports lymphocytes (the birds) by expressing lymphocyte survival factors (the fruit). During an immune response (the storm), the reticular cell (the tree) requires the help of dendritic cells (the men on the ground) to survive. The dendritic cells express lymphotoxin-β receptor ligands (the hands of the men), which modulate PDPN (the ropes). PDPN signals to promote activity of β1 integrins (the tree roots). β1-integrin-mediated cell-matrix adhesion (the tree staying rooted) helps the reticular cell to survive and function. Illustration drawn by Dragos Dasoveanu with assistance by Varsha Kumar.

Article

Immunity

A Dendritic-Cell-Stromal Axis Maintains Immune Responses in Lymph Nodes

Graphical Abstract

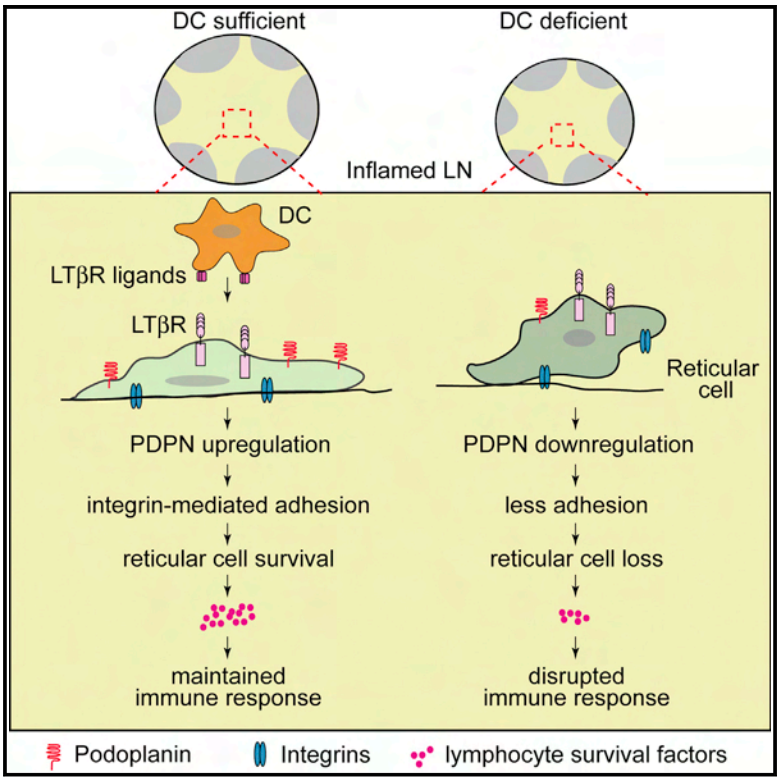

Highlights

- DCs maintain PDPN^{+} reticular cell survival during an ongoing immune response
- DCs maintain reticular cell survival via LTβR ligands
- LTβR signals modulate PDPN, which modulates cell adhesion needed for survival
- This DC-stromal axis maintains the ongoing immune response

Authors

Varsha Kumar,
Dragos C. Dasoveanu, ...,
Nancy H. Ruddle, Theresa T. Lu

Correspondence

lut@hss.edu

In Brief

Mesenchymal reticular cells modulate lymphocyte function in lymphoid tissues and can potentially be targeted in immune-mediated disease. Lu and colleagues show that, in activated lymph nodes, dendritic cells maintain reticular cell survival to maintain the ongoing immune response, which has implications for targeting inflamed lymphoid tissues in disease.

Kumar et al., 2015, Immunity *42*, 719–730
April 21, 2015
http://dx.doi.org/10.1016/j.immuni.2015.03.015

CellPress

Immunity
Article

A Dendritic-Cell-Stromal Axis Maintains Immune Responses in Lymph Nodes

Varsha Kumar,[1] Dragos C. Dasoveanu,[1] Susan Chyou,[1] Te-Chen Tzeng,[1,7] Cristina Rozo,[1] Yong Liang,[4] William Stohl,[5] Yang-Xin Fu,[4] Nancy H. Ruddle,[6] and Theresa T. Lu[1,2,3,*]
[1]Autoimmunity and Inflammation Program, Hospital for Special Surgery, New York, NY 10021, USA
[2]Pediatric Rheumatology, Hospital for Special Surgery, New York, NY 10021, USA
[3]Department of Microbiology and Immunology, Weill Cornell Medical College, New York, NY, 10021, USA
[4]Department of Pathology, Pritzker School of Medicine, University of Chicago, Chicago, IL 60637, USA
[5]Department of Rheumatology, Keck School of Medicine of USC, Los Angeles, CA 90033, USA
[6]Department of Epidemiology of Microbial Diseases, Yale School of Public Health, New Haven, CT 06520, USA
[7]Present address: University of Massachusetts, Worcester, MA 01655, USA
*Correspondence: lut@hss.edu
http://dx.doi.org/10.1016/j.immuni.2015.03.015

SUMMARY

Within secondary lymphoid tissues, stromal reticular cells support lymphocyte function, and targeting reticular cells is a potential strategy for controlling pathogenic lymphocytes in disease. However, the mechanisms that regulate reticular cell function are not well understood. Here we found that during an immune response in lymph nodes, dendritic cells (DCs) maintain reticular cell survival in multiple compartments. DC-derived lymphotoxin beta receptor (LTβR) ligands were critical mediators, and LTβR signaling on reticular cells mediated cell survival by modulating podoplanin (PDPN). PDPN modulated integrin-mediated cell adhesion, which maintained cell survival. This DC-stromal axis maintained lymphocyte survival and the ongoing immune response. Our findings provide insight into the functions of DCs, LTβR, and PDPN and delineate a DC-stromal axis that can potentially be targeted in autoimmune or lymphoproliferative diseases.

INTRODUCTION

Within lymph nodes, lymphocytes are supported by a non-hematopoietic vascular-stromal compartment that modulates lymphocyte survival, localization, and function (Cyster, 2005; Malhotra et al., 2013). Manipulating this compartment could be a means for controlling pathologic lymphocytes in autoimmune or lymphoproliferative diseases. As lymph nodes enlarge with stimulation, stromal reticular cells undergo a proliferative expansion (Chyou et al., 2011; Yang et al., 2014). Although initial proliferation and immune activation can potentially be targeted, patients with chronic immune diseases are likely to display ongoing responses. Understanding how reticular cells are maintained in already-enlarged nodes, then, can lead to the development of more effective therapeutic strategies.

Defined reticular cell populations in lymph nodes share the marker podoplanin (PDPN; also known as gp38) but serve distinct functions in each compartment. These cells are sometimes referred to as "fibroblastic reticular cells" (FRCs), although this term has been variably applied to all or different subpopulations (Chyou et al., 2011; Cremasco et al., 2014; Yang et al., 2014). Herein, we will use the descriptive term "PDPN$^+$ reticular cells" and refer to specific subsets when applicable. In the T zone, PDPN$^+$ reticular cells generate and ensheathe a network of collagen-rich fibrils, and the resulting reticular network facilitates T cell-dendritic cell (DC) interactions (Bajénoff et al., 2006; Malhotra et al., 2013). PDPN$^+$ reticular cells also express interleukin-7 (IL-7), which is required for naive T cell survival and CCL19 and CCL21, which compartmentalize T cells and DCs in the T zone (Cyster, 2005; Link et al., 2007). In contrast, B follicle reticular cells express CXCL13, which is required for B cell compartmentalization (Cyster, 2005; Katakai et al., 2008; Mionnet et al., 2013). CXCL13-expressing cells include follicular dendritic cells (FDCs) that present antigen to B cells, PDPN$^+$ marginal reticular cells (MRCs) that extend from the subcapsular sinus, and in secondary follicles, PDPN$^+$ reticular cells in the mantle zone at the border of the T and B zones. Mantle-zone PDPN$^+$ cells express BAFF (TNFSF13B), which supports naive B cell survival, and BAFF is also expressed in FDCs, where it can support germinal-center responses (Cremasco et al., 2014; Hase et al., 2004; Suzuki et al., 2010). In the medulla, PDPN$^+$ reticular cells presumably express CCL21 at low concentrations and CXCL12, which facilitates accumulation of plasmablasts and plasma cells (herein referred to collectively as "antibody-forming cells," [AFCs]) (Bannard et al., 2013; Braun et al., 2011; Hargreaves et al., 2001; Yang et al., 2014). CXCL12 might also promote AFC survival, and PDPN$^+$ cells can express interleukin-6 (IL-6), APRIL (TNFSF13), and other cytokines that might additionally contribute to AFC survival (Malhotra et al., 2013; Mohr et al., 2009). Directly depleting PDPN$^+$ reticular cells disrupts lymphocyte survival and ongoing immune responses (Cremasco et al., 2014; Denton et al., 2014), underscoring the potential utility of delineating reticular cell survival mechanisms.

The regulation of PDPN$^+$ reticular cell survival during ongoing immune responses is poorly understood. Endothelial and reticular cell proliferation begins within 2 days after immunization (Chyou et al., 2011; Yang et al., 2014). After immunization with ovalbumin (OVA) in complete Freund's adjuvant (CFA) or

stimulation with bone-marrow-derived dendritic cells, endothelial cell proliferation peaks on day 5 and is subsequently downregulated while endothelial cell numbers are maintained or continue to expand for at least another week. (Tzeng et al., 2010). The re-establishment of vascular quiescence is dependent on late-accumulating CD11c^{hi} cells presumed to be DCs (Tzeng et al., 2010). CD11c^{hi} cells are closely associated with perivascular reticular cells and maintain their tight organization around vessels, suggesting that late-accumulating DCs maintain aspects of reticular cell function. The re-establishment of vascular quiescence after day 5 parallels the development of germinal centers and AFCs, suggesting that understanding how DCs might regulate reticular cells throughout the lymph node could be helpful for manipulating ongoing immune responses.

Here we found that during the re-establishment of quiescence, DCs maintained reticular cell survival in multiple lymph node compartments. DC-derived lymphotoxin β receptor (LTβR) ligands were critical mediators of this effect, and the importance of these cell-associated ligands, the DC localization pattern, and the effect of DCs on reticular cell survival in vitro suggested that DCs act directly on reticular cells. LTβR signaling on reticular cells promoted survival by modulating PDPN, and PDPN signaling modulated integrin-mediated cell adhesion. In vivo, the effects of DCs, PDPN, and cell adhesion were observed during the re-establishment of quiescence but not during homeostasis, suggesting that this DC-stromal axis is specific to an inflamed environment. This axis maintained lymphocyte survival and the ongoing response. Together, our results identify new functions for DCs, LTβR, and PDPN in mediating reticular cell survival and establish a novel DC-stromal axis that can potentially be targeted in chronic immune diseases.

RESULTS

Non-T, Non-B CD11c^{+} Cells Localize with PDPN^{+} Cells in Multiple Compartments

To examine the effects of DCs on reticular cells in the context of robust B cell responses, we immunized mice with alum-precipitated OVA (OVA-Alum). Lymph node cellularity had increased by day 2 and was maximal by day 9 (Figure S1A). Similar to results obtained with other immunization strategies (Tzeng et al., 2010), endothelial cells showed peak proliferation on day 5 and relative quiescence on day 9 along with expanded numbers (Figure S1B–S1D). PDPN^{+} reticular cells showed similar proliferation and growth dynamics (Figure S1E–S1F), suggesting that the entire vascular-stromal compartment undergoes re-establishment of quiescence after day 5.

PDPN on reticular cells was upregulated over time (Figure S1G), and CD11c^{+} cells also accumulated. CD11c^{hi}MHCII^{med} (CD11c^{hi}) cells are presumed to be resident DCs, CD11c^{+}MHCII^{hi} (MHCII^{hi}) cells include DCs recruited from skin and blood, and CD11c^{med}MHCII^{med} (CD11c^{med}) cells include monocytes, macrophages, plasmacytoid DCs, and inflammatory DCs (Merad et al., 2013; Tzeng et al., 2010). CD11c^{med} and MHCII^{hi} cells were highly enriched by day 2 (Figures S1H and S1I), reflecting the rapid accumulation of interleukin-1β-expressing monocytes and MHCII^{hi} DCs that can help drive early vascular-stromal proliferation (Benahmed et al., 2014). MHCII^{hi} DCs remained enriched on day 9 but had a less activated phenotype, with reduced MHCII and CD11b expression (Figures S1H and S1I and data not shown). CD11c^{hi} cells, in contrast to the other populations, accumulated more slowly; the greatest enrichment occurred on day 9 (Figure S1H and S1I). Re-establishment of vascular-stromal quiescence, then, was associated with high reticular cell PDPN and maximal accumulation of CD11c^{hi} DCs.

To study the localization and function of non-T, non-B CD11c^{+} cells (Baumjohann et al., 2013; Jung et al., 2002; Tzeng et al., 2010), we generated *Cd11c*$^{-DTR}$*Rag1*$^{-/-}$ mixed chimeras whereby lethally irradiated wild-type (WT) recipients were reconstituted with 80% *Cd11c*$^{-DTR}$*Rag1*$^{-/-}$ and 20% WT bone marrow (Figure S2). In these chimeras, non-T, non-B CD11c^{+} cells were marked by the expression of the DTR-EGFP fusion protein, At day 9 after immunization, EGFP^{+} cells were found throughout the T zone and also in B cell areas (Figures 1A and 1B). In the T zone, EGFP^{+} cells were closely associated with the network of PDPN^{+} cells and fibrils marked by ER-TR7 antibody (Figure 1C). In secondary follicles, EGFP^{+} cells were located within the mantle zone at the T-B border, where they were associated with PDPN^{+} cells (Figures 1D and 1E). EGFP^{+} cells were also located in other areas of the mantle zone and within germinal centers (Figure 1D). Consistent with findings from CD11c staining (Mohr et al., 2009; Tzeng et al., 2010), EGFP^{+} cells also localized within the medullary cords with CD138^{+} AFCs (Figure 1F) and were associated with PDPN^{+} reticular cells (Figure 1F). Together, these chimeras suggested that non-T, non-B CD11c^{+} cells were associated with PDPN^{+} reticular cells in multiple compartments.

Non-T, Non-B CD11c^{+} Cells Maintain Reticular Cell Numbers and the Ongoing Immune Response

Diphtheria toxin (DT) treatment of the *Cd11c*$^{-DTR}$*Rag1*$^{-/-}$ chimeras depleted CD11c^{hi} cells by 80% and MHCII^{hi} DCs by about 50% (Figure 2A). Blood endothelial cell ICAM-1 was upregulated (Figure S3A), consistent with previous findings (Tzeng et al., 2010). PDPN^{+} reticular cell numbers were partially reduced without a concomitant increase in PDPN^{-} reticular cells (Figure 2B), suggesting the possibility of disrupted PDPN^{+} reticular cell survival. CD11c^{+} cell depletion also reduced lymph node cellularity and the numbers of total B and T cells, germinal center B cells, and IgG^{+} AFCs (Figures 2C–2E). Activated CD4^{+} T cell percentages and regulatory T cell percentages were not altered (Figures S3B and S3C). CD11c^{+} cell depletion reduced lymphocyte numbers even upon blockade of lymph node entry and exit (Figure S3D), suggesting that lymphocyte loss was due to compromised survival. We did not detect more AFCs in the blood circulation or bone marrow (Figure S3E), suggesting that the AFC loss was due not to lymph node egress but to disrupted AFC survival. These results together suggested that CD11c^{+} cells maintain PDPN^{+} reticular cell numbers and the ongoing immune response.

Classical DCs Maintain Reticular Cell Survival and the Ongoing Immune Response

To understand whether the effects of CD11c^{+} cell depletion primarily reflected the depletion of DCs, we used *Zbtb46*-EGFP reporter mice and zDC-DTR mice that express diphtheria toxin receptor in Zbtb46-expressing cells. Zbtb46 is a transcription

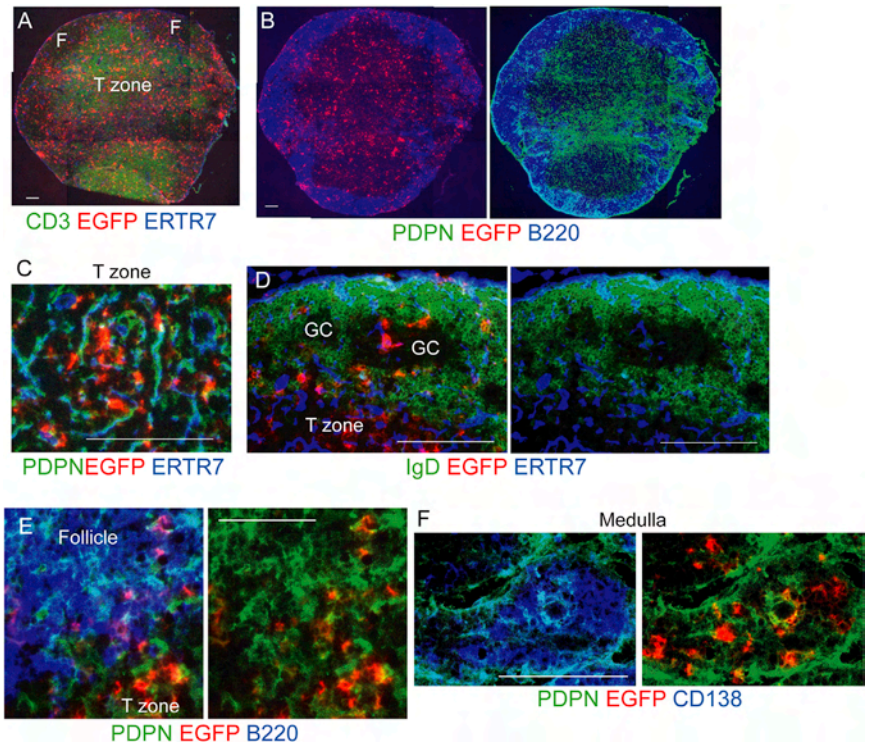

Figure 1. Non-T, Non-B CD11c$^+$ Cells Localize with PDPN$^+$ Cells in Multiple Compartments

Cd11c^{-DTR}*Rag1*$^{-/-}$ mixed chimeras were immunized in footpads with OVA-alum on day 0, and draining popliteal nodes were taken on day 9. Sections were stained for the DTR-EGFP fusion protein and other indicated markers. (A and B) Nearby sections from the same lymph node showing EGFP$^+$ cell localization relative to (A) T cells and (B) B cells and PDPN$^+$ cells. F = follicle. (C–F) EGFP$^+$ cell localization in the (C) T zone, (D) follicles (GC = germinal center), (E) follicular mantle zone, and (F) medulla. Results are representative of at least three lymph nodes. (A, B, D, and F) The scale bar represents 100 μm. (C and E) The scale bar represents 50 μm. See also Figures S1 and S2.

factor also expressed by endothelial cells, and it distinguishes classical Flt3-dependent DCs from monocytes and monocyte-derived cells (Meredith et al., 2012; Satpathy et al., 2012). *Zbtb46*-EGFP mice (Satpathy et al., 2012) confirmed DC localization in the T zone, within the mantle zone at the T-B boundary, and more sparsely in the rest of the mantle zone and in germinal centers (Figure S4A). To deplete DCs without depleting endothelial cells, we generated zDC-DTR→WT chimeras. Similar to CD11c$^+$ cell depletion, DT treatment of these chimeras depleted the vast majority of CD11c^{hi} cells and partially depleted the MHCII^{hi} population (Figure 3A). CD11c^{med} cells were also partially depleted (Figure 3A). As with CD11c$^+$ cell depletion, DC depletion reduced PDPN$^+$ reticular cell numbers without increasing PDPN$^-$ cells (Figure 3B). PDPN$^+$ reticular cell loss was accompanied by an increased percentage of TUNEL$^+$ cells (Figure 3C), suggesting that the cell loss was due to disrupted survival. To understand whether DC depletion disrupted reticular cell survival in multiple compartments, we stained reticular cells intracellularly for CCL21 to identify T zone and medullary cells and for CXCL13 to identify follicular cells (Figure S4B). CCL21$^-$CXCL13$^-$ cells that most likely included medullary cells were calculated by subtracting CCL21$^+$ and CXCL13$^+$ cell numbers from total PDPN$^+$ cell numbers. Such subsetting showed that CCL21$^+$ cells comprised the largest subpopulation on day 9 (Figure S4B). FDCs were identified by CD35 staining and were both PDPN$^+$ and PDPN$^-$ (Figure S4C) (Jarjour et al., 2014; Link et al., 2007). PDPN$^+$ FDCs were partially CXCL13$^+$ and partially CCL21$^+$ (Cremasco et al., 2014; Wang et al., 2011) and comprised 20%–35% of each PDPN$^+$ subpopulation (Figure S4C). Upon DC depletion, each of the PDPN$^+$ CCL21$^+$, CXCL13$^+$, CCL21$^-$CXCL13$^-$ subpopulations was reduced in number (Figure 3D), whereas the proportions of CD35$^+$ cells (i.e., FDCs) and CD35$^-$ cells in each subpopulation stayed constant (Figure S4C). This suggested that reticular cells in the T zone, follicular mantle, and medulla along with PDPN$^+$ FDCs were lost with DC depletion. Total (PDPN$^+$ and PDPN$^-$) FDCs were also reduced in number (Figure 3D). These results suggested that DCs maintain the survival of PDPN$^+$ reticular cells in the T zone, follicular mantle, and medulla and of FDCs in germinal centers.

DC depletion also reduced the numbers of B and T cells, germinal center B cells, and AFCs (Figures 3E and 3F). Lymphocyte staining by TUNEL (terminal deoxynucleotidyl transferase dUTP nick-end labeling) was increased (Figure 3G), supporting the idea of disrupted lymphocyte survival. Morphologically, follicles with germinal centers were present (Figure S4D), although the number of germinal centers was reduced (Figure 3H). Numbers of activated caspase 3$^+$ cells were increased (Figure S4E), suggesting disrupted germinal-center B cell survival. There was greater mixing of CD8$^+$ T cells with IgD$^+$ B cells at the T-B border (Figure 3I and Figure S4F), suggesting that reticular cells in this region were among the mantle-zone cells lost. DC depletion during homeostasis did not affect PDPN$^+$ reticular or lymph node cell numbers (Figure S4G). These results indicated that classical DCs maintain reticular cell survival, integrity of lymph node compartments, and the ongoing immune response in stimulated lymph nodes.

CD11c$^+$ Cells Maintain Stromal-Derived Lymphocyte Survival-Factor Expression

The disrupted lymphocyte survival associated with DC depletion led us to ask about survival-factor expression. B cells in CD11c$^+$-cell-depleted nodes had higher expression of the BAFF receptor (Figure 4A), suggesting reduced BAFF availability (Lesley et al., 2004). PDPN$^+$ reticular cells on day 9 expressed high amounts of BAFF, IL-6, and IL-7 relative to amounts expressed by other vascular-stromal cells and to CD11c$^+$ cells (Figures 4B and 4C). Upon CD11c$^+$ cell depletion, amounts of PDPN$^+$ reticular cell BAFF, IL-6, and IL-7 were all reduced (Figure 4D), consistent with the loss of reticular cells

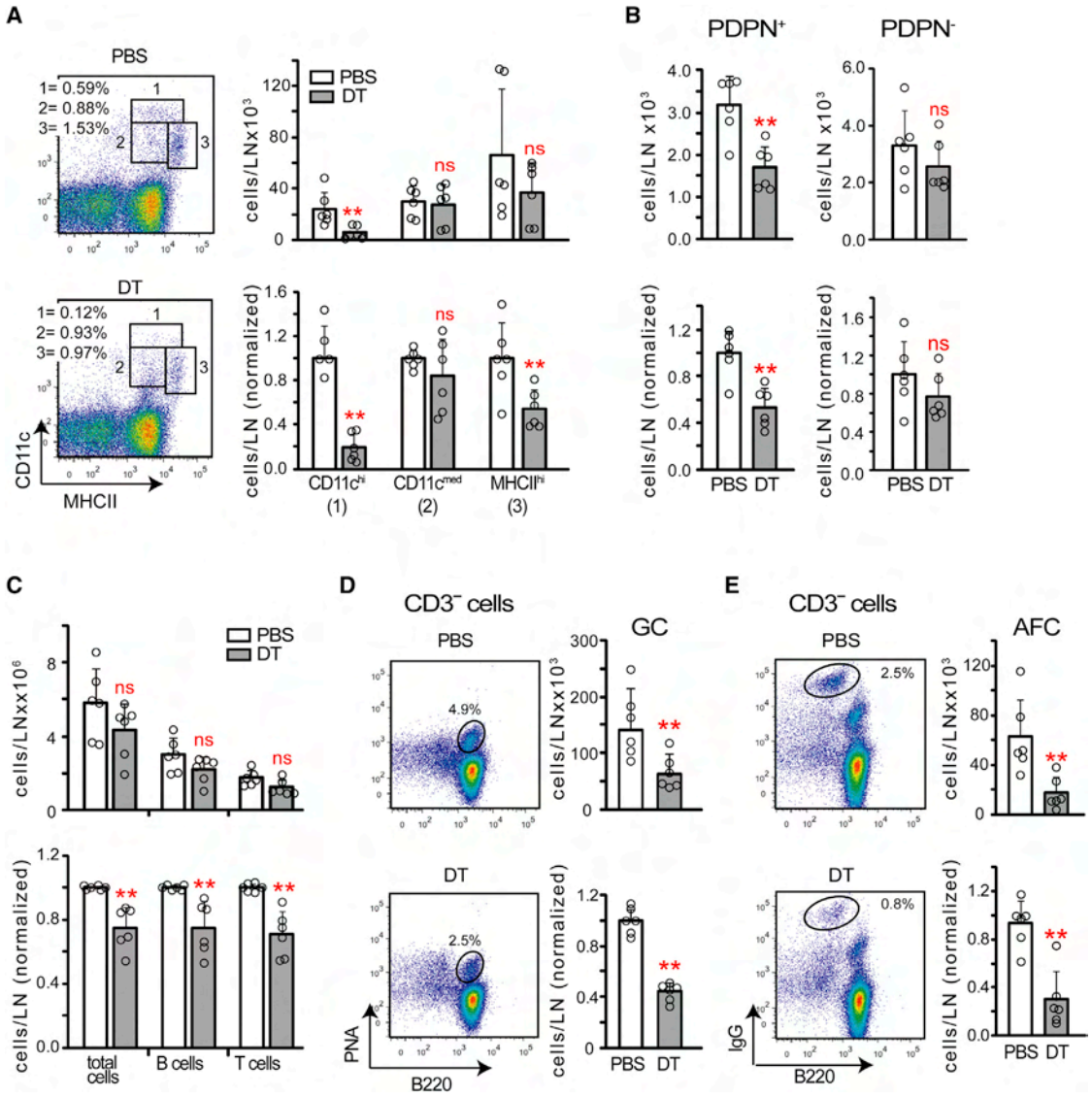

Figure 2. Non-T, Non-B CD11c⁺ Cells Maintain PDPN⁺ Reticular Cells and the Ongoing Immune Response

Cd11c^{-DTR}*Rag1*$^{-/-}$ mixed chimeras were immunized on day 0, treated with PBS or DT on day 8, and examined on day 9.

(A) CD11c⁺ cell numbers. Left: representative flow-cytometry plots. Right: absolute and relative numbers.

(B and C) Absolute and relative numbers of (B) PDPN⁺ and PDPN⁻ reticular cells and (C) total, B220⁺ B, and CD3⁺ T cells.

(D and E) Left: representative flow-cytometry plots. Right: absolute and relative numbers of (D) germinal-center B cells and (E) AFCs.

Data were pooled from 3–4 independent experiments. Each point represents one mouse; error bars represent SD. ** $p < .01$ in an unpaired t test comparing DT to PBS samples. See also Figure S3.

in multiple compartments. These results suggested that DC depletion led to reduced stromal expression of lymphocyte survival factors; along with a loss of DC-derived survival factors (Mohr et al., 2009), this reduced expression contributed to disruption of the immune response.

DC-Derived LTβR Ligands Maintain Reticular Cells

LTβR can modulate stromal function, and lymph node CD11c⁺ cells can express LTβR ligands (Boulianne et al., 2012; Lu and Browning, 2014; Moussion and Girard, 2011; Zhu et al., 2011). LTβR-Ig reduced PDPN⁺ reticular cell numbers (Figure 5A), suggesting that DCs could maintain reticular cell survival via LTβR ligands α1β2 and LIGHT (TNFSF14). CD11c⁺ cells expressed less LTα and LTβ than did unfractionated lymph node cells (Figure 5B), reinforcing the idea that lymphocytes are major sources of LTα1β2 (Junt et al., 2006) but not excluding the potential importance of DC-derived LTα1β2. CD11c⁺ cells, on the other hand, expressed more LIGHT than unfractionated lymph nodes (Figure 5B). We tested the importance of DC-derived LTα1β2 and LIGHT by reconstituting wild-type mice with a mix of zDC-DTR and WT bone marrow or substituted the WT bone marrow with *Ltb*$^{-/-}$*Rag1*$^{-/-}$ or *Tnfsf14*$^{-/-}$*Rag1*$^{-/-}$ bone marrow (Figure S5A). All T and B cells in these chimeras were LTβ- or LIGHT-sufficient, and DT treatment on day 8 after immunization

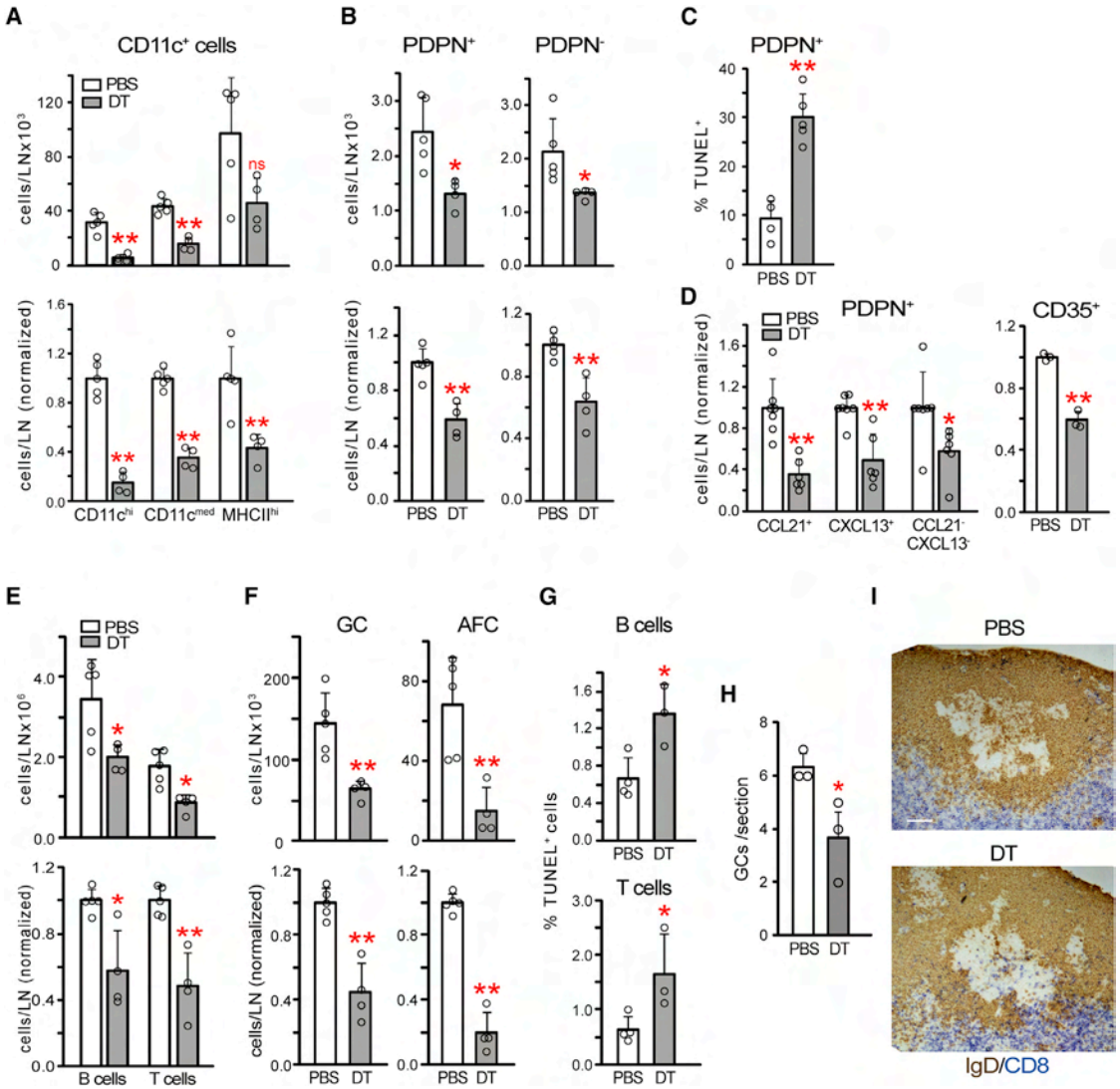

Figure 3. Classical DCs Maintain Reticular Cell Survival and the Ongoing Immune Response

zDC-DTR chimeras were immunized on day 0, injected with PBS or DT on day 8, and examined on day 9.

(A) CD11c$^+$ cell numbers. Data were pooled from three experiments.

(B) PDPN$^+$ and PDPN$^-$ reticular cell numbers. Data were pooled from four experiments.

(C) PDPN$^+$ reticular cell TUNEL staining, expressed as a percentage of PDPN$^+$ reticular cells that are TUNEL$^+$. Data were pooled from two experiments.

(D) Reticular cell subpopulation numbers. Left: normalized numbers of indicated PDPN$^+$ reticular cell subsets. Data are from four experiments. Right: normalized numbers of total (PDPN$^+$ and PDPN$^-$) CD35$^+$ cells. Data are from two experiments.

(E and F) B and T cell (E) and germinal-center B cell and AFC (F) numbers. Data are from three experiments.

(G) TUNEL staining in B220$^+$ B cells and (CD45$^+$) Thy1$^+$ T cells. Data were pooled from two experiments.

(H) Number of germinal centers per tissue section. Data were pooled from three experiments.

(I) Compartmental integrity. Representative of at least three pairs of mice. The white bar represents 100 μm. For (A–H), each symbol represents one mouse; error bars represent SD. *p < .05 and **p < .01 in an unpaired t test comparing DT and PBS samples. See also Figure S4.

resulted in DCs that had relative LTβ or LIGHT deficiency in the experimental groups (Figure S5B). Lymph node cellularity was similar across groups before depletion, and reticular cell numbers were actually greater in LTβ-deficient chimeras (Figures S5C and S5D), but DT treatment reduced total numbers of PDPN$^+$ reticular cells specifically in the LTβ- and LIGHT-deficient chimeras (Figure 5C). LTβ deficiency affected each of the CCL21$^+$, CXCL13$^+$, and CCL21$^-$CXCL13$^-$ subpopulations (Figure 5C). The reduction in the LIGHT-deficient chimeras was more variable and reached statistical significance only in the CCL21$^-$CXL13$^-$ subset (Figure 5C). These results suggest that both DC-derived LTα1β2 and LIGHT maintain PDPN$^+$ reticular cell survival.

In vitro, CD11c$^+$ cells maintained the survival of serum-starved PDPN$^+$ reticular cells (Figure S5E, left and middle). This effect was blocked by LTβR-Ig (Figure S5E, left and middle), further supporting the concept that DCs express LTβR ligands to maintain reticular cell survival.

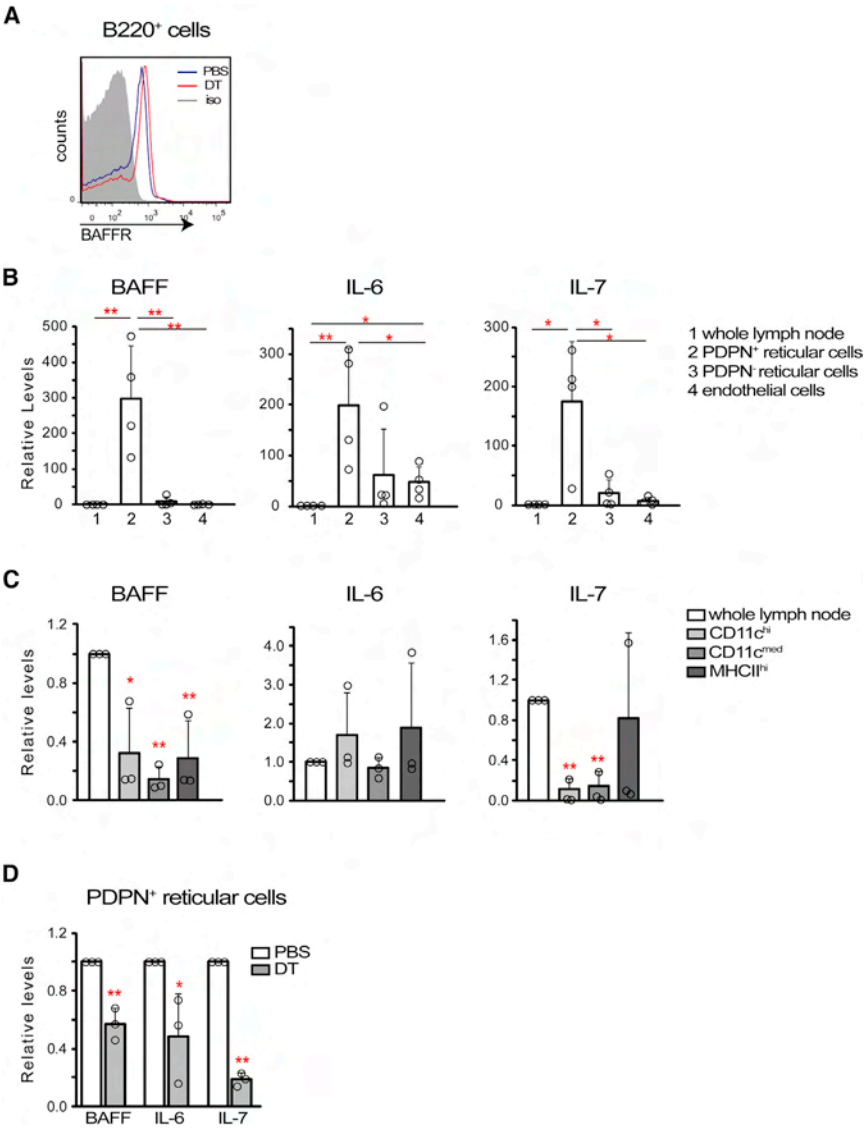

Figure 4. CD11c⁺ Cell Depletion Reduces Stromal Expression of Lymphocyte Survival Factors

Mice were immunized on day 0 and treated or examined at indicated time points after immunization.

(A) B cell BAFF receptor expression in *Cd11c*$^{-DTR}$*Rag1*$^{-/-}$ chimeras given PBS or DT on day 8 and examined on day 9. Data are representative of three pairs of mice from two experiments.

(B and C) Expression of BAFF, IL-6, and IL-7 by (B) vascular-stromal and (C) CD11c⁺ cell subsets. Indicated populations were sorted from (B) day 9 or (C) day 8 draining nodes, and cytokine expression was evaluated by qPCR. "Whole lymph node" indicates collagenase-digested lymph node cells prior to cell separation. Note differences in scale in (B) and (C). Data were pooled from (B) four and (C) three independent experiments.

(D) Cytokine expression by PDPN⁺ reticular cells on day 9 after CD11c⁺ cell depletion on day 8 in CD11c-DTR mice. Data were pooled from three independent experiments.

For (B–D), each symbol represents one sample sorted from (B and D) 6–8 mice or (C) 4–5 mice. *p < .05 and **p < .01 in an unpaired t test comparing the indicated cells with controls or as indicated. Error bars represent SD.

PDPN Maintains Reticular Cell Survival and the Ongoing Immune Response

We noted a drop in reticular cell PDPN expression upon DC depletion (Figure 6A), and a drop was detectable as early as 5.5–8 hr after DT injection in association with increased apoptosis (Figure S6A). In vitro, CD11c⁺ cells induced PDPN upregulation, which was blocked by LTβR-Ig (Figure S5E, right). These data suggest the possibility that DCs modulated PDPN to maintain reticular cell survival.

We asked whether PDPN mediated reticular cell survival by treating mice with PDPN-targeted siRNA on days 6 and 7 after immunization and analyzing results on day 9. In initial experiments involving labeled siRNA, about 30% of PDPN⁺ reticular cells in draining nodes were labeled, whereas only 5% of cells were labeled in non-draining nodes (data not shown), potentially reflecting differential blood flow. By day 9, PDPN-targeted siRNA had reduced PDPN⁺ reticular cell numbers (Figure 6B) and increased TUNEL staining (Figure 6C). As occurred after DC depletion, CCL21⁺, CXCL13⁺, and CCL21⁻CXCL13⁻ populations and total numbers of FDCs were reduced upon PDPN targeting (Figure 6D). These results suggested that PDPN maintained reticular cell survival in immunized nodes.

PDPN targeting also reduced B and T cell, germinal center B cell, and AFC numbers (Figures 6E and 6F) and increased lymphocyte TUNEL staining (Figure 6G). Germinal centers were fewer in number, and CD8⁺ T cells and IgD⁺ B cells mixed at the T-B boundary (Figures S6B and S6C). PDPN⁺ reticular cells expressed less BAFF and IL-7 upon PDPN knockdown (Figure 6H). These results suggest that, similar to DC depletion, PDPN knockdown disrupted the ongoing immune response, potentially by disrupting reticular cell survival and reducing lymphocyte survival-factor expression.

Because PDPN is also expressed on lymphatic endothelial cells and myeloid cells (Astarita et al., 2012; Schacht et al., 2003), we asked whether PDPN on reticular cells directly modulated cell survival. PDPN knockdown in cultured reticular cells reduced cell numbers (Figure 6I) and increased annexin V staining (Figure 6J), echoing the increased apoptosis seen in vivo. In serum-starved cultures, agonist anti-LTβR treatment increased PDPN expression and cell numbers (Figure 6K). However, PDPN knockdown prevented the increase in cell numbers (Figure 6K), supporting the idea that DC-derived LTβR ligands mediate reticular cell survival via PDPN.

We next examined how PDPN mediated cell survival. PDPN activates Rho GTPases and modulates phosphorylation of the

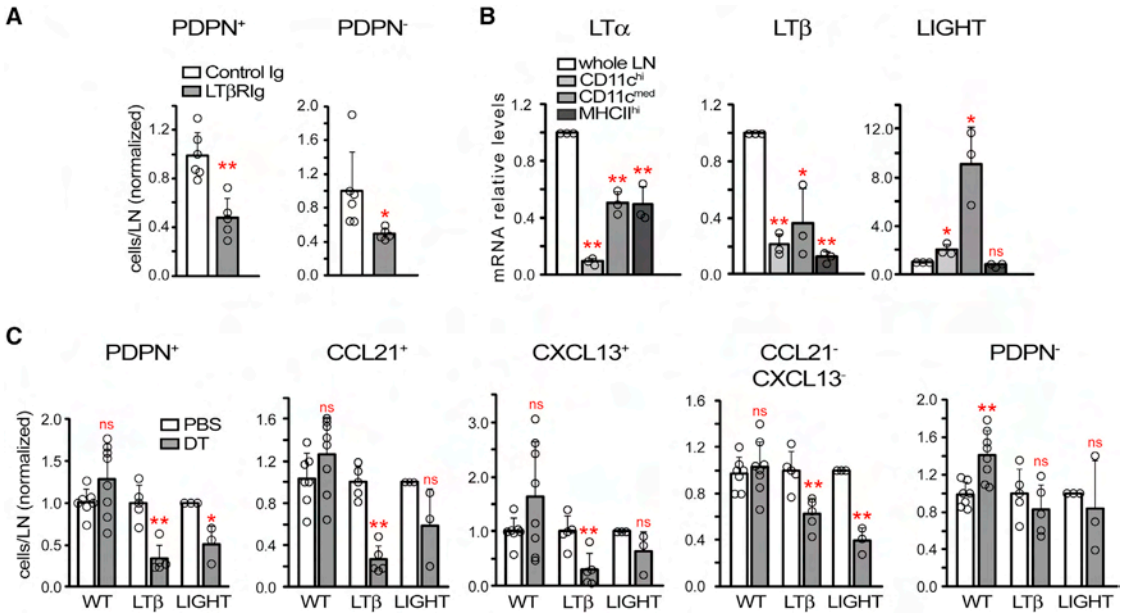

Figure 5. DC-Derived LTβR Ligands Maintain Reticular Cells

Mice were immunized on day 0 and treated or examined at the indicated time points after immunization.

(A) PDPN$^+$ and PDPN$^-$ reticular cell numbers in mice treated with LTβR-Ig on day 8 and examined on day 9. Data were pooled from two experiments.

(B) LTβR ligand mRNA expression by "whole" unsorted lymph node cells and the indicated CD11c$^+$ cell subsets on day 8. Data are from three experiments.

(C) Role of DC-derived LTβR ligands. zDC-DTR: WT, LTβ-, or LIGHT-deficient mixed chimeras were immunized on day 0 and given PBS or DT on day 8, and reticular cell subset numbers were analyzed on day 9. Data are from three separate experiments for both LTβ- and LIGHT-deficient chimeras.

For (A and C), each symbol represents one mouse. For (B), each symbol represents one sample sorted from 4–5 pooled mice. *p < .05 and **p < .01 in an unpaired t test comparing the indicated samples. Error bars indicate SD. See also Figure S5.

ezrin, radixin, moesin (ERM) family of cytoplasmic signaling proteins that link membrane receptors to the cytoskeleton (Acton et al., 2014; Astarita et al., 2015; Martín-Villar et al., 2006). This signaling was recently found to mediate cell contractility in lymph node reticular cells (Acton et al., 2014; Astarita et al., 2015). Consistent with this PDPN signaling pathway, PDPN knockdown reduced the amount of phosphorylated ERM (pERM) (Figure 6L). The extracellular domain of PDPN can associate with a number of cell-surface molecules, and this domain might be key for mediating ERM phosphorylation (Astarita et al., 2012; Astarita et al., 2015); adding PDPN-Fc to disrupt PDPN interactions with other membrane proteins also resulted in reduced cell numbers and pERM (Figure S6D). CLEC-2 on DCs can bind PDPN and act as an antagonist (Acton et al., 2014; Astarita et al., 2015), but CLEC-2-Fc effects can be transient in vitro (Acton et al., 2014) and had not influenced cell numbers by 48 hr after CLEC2-Fc treatment (Figure S6E). In vivo, DC depletion reduced reticular cell pERM (Figure S6F). ERM phosphorylation and cell contraction downstream of PDPN are blocked in vitro by the Rho kinase (ROCK) inhibitor Y27632 (Acton et al., 2014; Astarita et al., 2015; Martín-Villar et al., 2006), and Y27632 also disrupted cell survival (Figure 6M). Together, these results suggest that PDPN mediates reticular cell survival via the same Rho-ROCK-ERM pathway that mediates cell contractility.

Cell contractility is linked to cell-matrix adhesion, which can modulate cell survival (Geiger et al., 2009). PDPN is a positive regulator of cell adhesion (Astarita et al., 2015; Schacht et al., 2003), and PDPN knockdown reduced cell adhesion (Figure 6N). Blocking β1 integrins reduced cell survival (Figure 6O), suggesting that cell-matrix adhesion was important for cell survival in our system. Focal adhesion kinase (FAK) phosphorylated at Y397 is a major transducer of integrin-mediated cell-survival signals (Mitra and Schlaepfer, 2006), and PDPN knockdown reduced pFAK phosphorylation at Y397 (Figure 6P). Similar to PDPN knockdown, anti-PDPN reduced cell survival and amounts of phospho-FAK (pFAK) (Figure S6G). ROCK inhibition also reduced pFAK amounts (Figure 6Q), establishing linked regulation of contractility and adhesion in these cells. In vivo, DC depletion reduced amounts of pFAK (Figure S6H). Together, these results suggested that PDPN mediates cell survival at least in part via Rho and modulation of integrin-mediated cell adhesion.

Consistent with the in vivo PDPN-knockdown results, administration of anti-PDPN on day 8 after immunization had reduced reticular cell numbers by day 9 (Figure S6I). In contrast, anti-PDPN in homeostatic mice for 24 hr did not reduce cell numbers (Figure S6I), echoing the recent finding that anti-PDPN for 48 hr during homeostasis increases reticular cell proliferation (Astarita et al., 2015). These results suggested that PDPN plays different roles in homeostatic and stimulated lymph nodes. We asked whether these context-dependent differences could be related to differences in cell adhesion. pFAK was upregulated along with PDPN by day 9 after immunization (Figure 6R and Figure S1G), suggesting upregulation of cell adhesion. Cell-adhesion upregulation can be a survival mechanism in that it counters the pro-apoptotic effects of TNFα or other insults (Fornaro et al.,

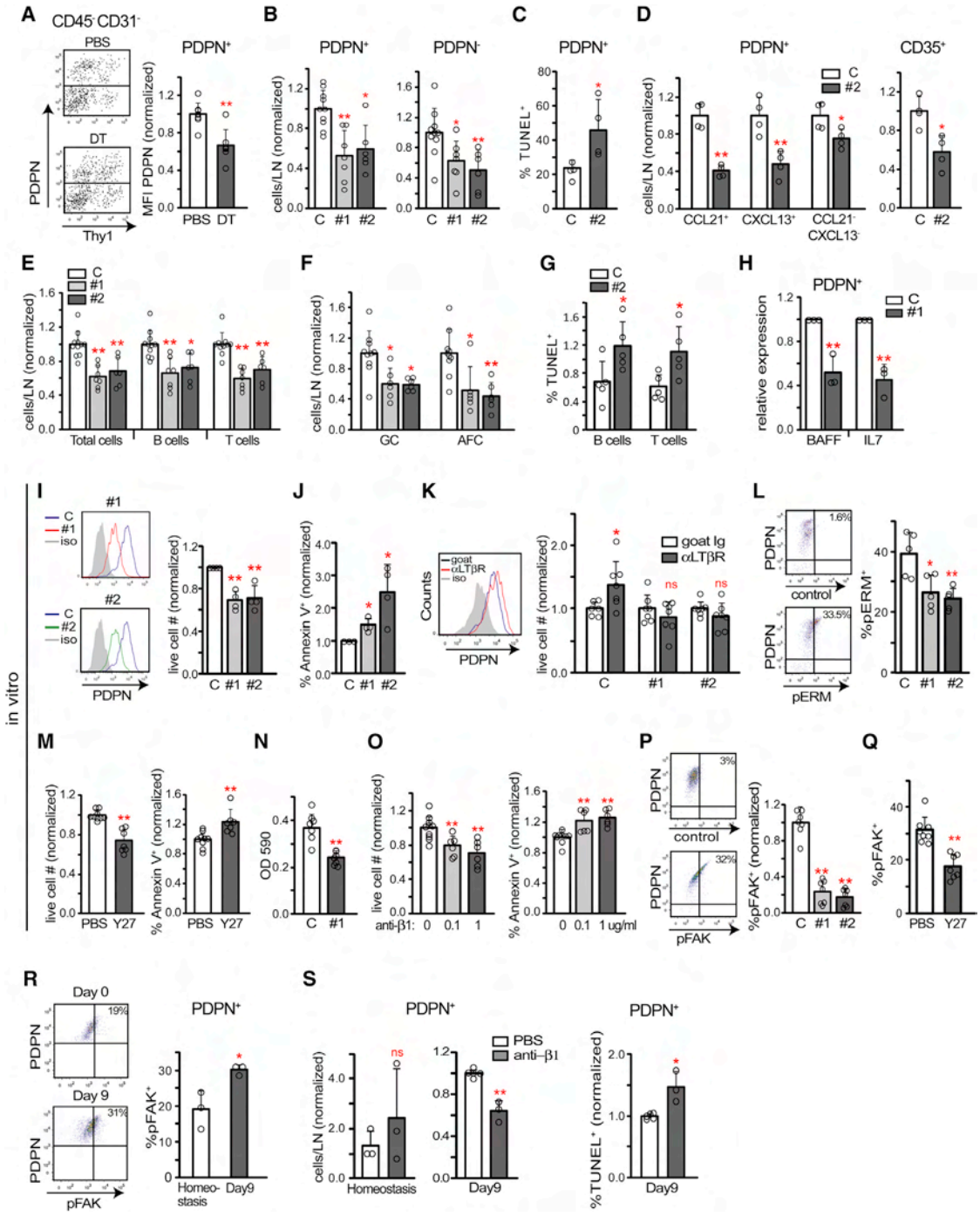

Figure 6. PDPN on Reticular Cells Is Regulated by DCs and Maintains Cell Survival

(A) PDPN expression on PDPN$^+$ reticular cells in zDC-DTR chimeras 24 hr after DC depletion. Left: representative flow-cytometry plots. Right: pooled analysis of PDPN geometric mean fluorescence intensity from five experiments.

(B–H) Mice were immunized on day 0 and injected with control or indicated PDPN-targeted siRNAs (PDPN #1 or PDPN #2) on days 6 and 7, and draining popliteal nodes were examined on day 9. (B) PDPN$^+$ and PDPN$^-$ reticular cell numbers. Data were pooled from at least three experiments. (C) PDPN$^+$ reticular cell TUNEL expression. Data were pooled from two experiments. (D) Relative numbers of indicated subsets of PDPN$^+$ reticular cells and of total (PDPN$^+$ and PDPN$^-$) CD35$^+$ cells. Data were pooled from two experiments. (E and F) Relative numbers of (E) total, B, and T cells and (F) germinal-center B cells and AFCs. Data are from at least three experiments. (G) B and T cell TUNEL staining. Data are from two experiments. (H) mRNA expression of the indicated cytokines by sorted PDPN$^+$ reticular cells. Each symbol represents one sample sorted from eight mice; there was one sample per condition per experiment.

(I–L) Cultured PDPN$^+$ reticular cells were transfected with control, PDPN#1, or PDPN#2 siRNA. (I) Left: histograms showing the extent of PDPN knockdown. Right: relative cell counts of live gated cells 48–72 hr after transfection. Data were pooled from four experiments; there was one well per condition per experiment. (J)

(legend continued on next page)

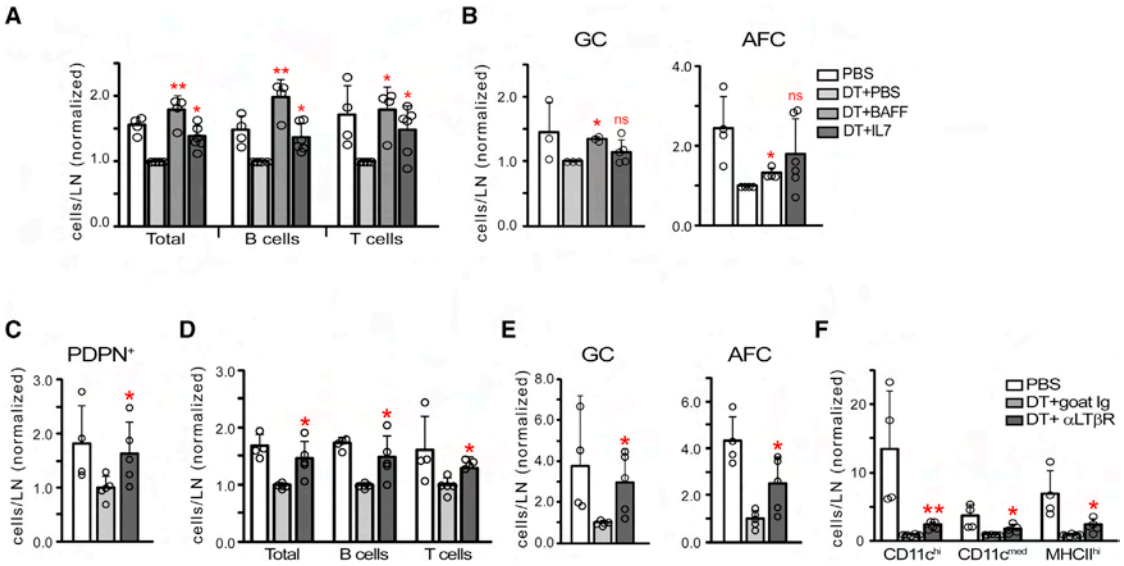

Figure 7. Disrupted Immune Responses after DC Depletion Can Be Rescued by Administration of Survival Factors or Stimulation with LTβR

(A and B) BAFF and IL-7 administration. zDC-DTR chimeras were given PBS or DT on day 8 after immunization and the indicated cytokine 5–8 hr after PBS or DT administration. Mice were examined 20–24 hr after cytokine injection. The numbers of cells in the indicated populations were normalized and compared to "DT + PBS" numbers. (A) Total, B, and T cell numbers. (B) Germinal-center B cell and AFC numbers. Data are from four experiments.

(C–F) LTβR stimulation. The experimental setup was the same as in (A and B) except that zDC-DTR chimeras received control goat Ig or agonist anti-LTβR after DT administration. The numbers of indicated populations were normalized and compared to "DT + goat Ig" numbers. (C) PDPN$^+$ reticular cells. (D) Total, B, and T cells. (E) Germinal-center B cells and AFCs. (F) CD11c$^+$ cell subsets. Data are from four experiments

Each symbol represents one mouse. *p < .05 and **p < .01 in an unpaired t test comparing mice to the indicated controls. Error bars indicate SD. See also Figure S7.

2003), and we asked whether adhesion was more important for cell survival in inflamed lymph nodes than in homeostatic ones. Indeed, β1 integrin-blocking antibody had reduced PDPN$^+$ reticular cell survival on day 9 after immunization but not during homeostasis (Figure 6S). These results suggested that PDPN during the re-establishment of quiescence maintains a level of cell-matrix adhesion that permits reticular cell survival.

Survival-Factor Supplementation or LTβR Stimulation Rescues the Immune Response upon DC Depletion

We tested the extent to which the loss of survival factors contributed to the lymphocyte loss in DC-depleted mice. BAFF rescued total B and germinal-center B cell numbers (Figure 7A), supporting the idea that DC depletion reduced the numbers of BAFF-expressing mantle-zone reticular cells and FDCs. T cell numbers

Annexin V binding. The percent of DAPI$^-$ or 7AAD$^-$ cells that were Annexin V$^+$ was normalized to control siRNA samples. Each symbol represents one well; data were pooled from three experiments, and there were 1–2 wells per condition per experiment. (K) Effects of LTβR stimulation. 48 hr after transfection, media were changed to serum-free media with goat IgG or anti-LTβR. Live-gated cells were analyzed 24 hr later. Left: PDPN expression in control siRNA samples. Right: cell numbers, normalized to the goat IgG sample. Each symbol represents one well; data were pooled from four experiments, and there were 1–3 wells per condition per experiment. (L) pERM expression. Cells were examined 48 hr after transfection. Left: representative flow-cytometry plots of control siRNA cells. Right: pERM levels expressed as a percentage of cells that are pERM$^+$. Each symbol represents one well; data were pooled from two experiments, and 2–3 samples per condition per experiment were included.

(M) Effects of Y27632 treatment on cell survival. Left: numbers of DAPI$^-$ cells. Right: Annexin V binding on DAPI$^-$ cells. Each symbol represents one well; data were pooled from two of four similar experiments, and there were 3–5 wells per condition per experiment.

(N) Cell adhesion upon PDPN knockdown, shown as OD at 590 nm. Each symbol represents one well; data were pooled from three experiments, and there were 2–3 wells per condition per experiment.

(O) Effect of β1 integrin blockade on cell survival. Left: numbers of DAPI$^-$ cells. Right: Annexin V binding on DAPI$^-$ cells. Each symbol represents one well; data were pooled from two experiments, and there were 3–5 wells per condition per experiment.

(P) pFAK (at Y397) expression with PDPN knockdown. Cells were examined 48 hr after transfection. Left: representative flow-cytometry plot of control siRNA cells. Right: pFAK expression. The percent of cells that are pFAK$^+$ was normalized to control siRNA samples. Each symbol represents one well; data were pooled from three experiments, and there were 2–3 wells per condition per experiment.

(Q) Reticular cell pFAK expression upon Y27632 treatment. Each symbol represents one well; data were pooled from two experiments, and there were 2–3 wells per condition per experiment.

(R) PDPN$^+$ reticular cell pFAK expression during homeostasis and on day 9 after immunization. Left: representative flow-cytometry plots. Right: pFAK expression. Each symbol represents one mouse; data were pooled from two experiments.

(S) Effect of β1 integrin blockade for 24 hours in vivo. Left: PDPN$^+$ reticular cell numbers during homeostasis and on day 9 after immunization. Right: TUNEL staining in day 9 mice. Each symbol represents one mouse; data are from two (homeostasis) to three (day 9) experiments.

*p < .05 and **p < .01 in an unpaired t test comparing treated cells to the indicated controls. Error bars indicate SD. See also Figure S6.

were also rescued (Figure 7A), perhaps in part reflecting T cell responses to BAFF (Mackay and Leung, 2006). AFC numbers were partially rescued (Figure 7B), suggesting roles for additional factors. IL-7 rescued T cell numbers (Figure 7A), consistent with the loss of IL-7-expressing T zone reticular cells. IL-7 also rescued total B cell numbers (Figure 7A), potentially reflecting a role for IL-7 in the medulla or follicles (Link et al., 2007). BAFF and IL-7 supplementation had similar effects when PDPN was knocked down (Figure S7A). These results together support the idea that reduced stromal-derived survival factor, probably in combination with the loss of DC-derived factors (Mohr et al., 2009), contributed to the disrupted immune response in DC-depleted mice.

We asked whether preventing reticular cell loss despite DC depletion could prevent lymphocyte loss. On day 8 after immunization, zDC-DTR chimeras were treated with DT and, 5.5–8 hr later, with control or agonist LTβR antibody. Anti-LTβR prevented the DT-induced reduced numbers of PDPN$^+$ reticular cells, B cells, T cells, and germinal-center cells and partially prevented the loss of AFCs (Figures 7C–7E). CD11c$^+$ cell numbers were modestly increased with anti-LTβR, but the numbers were still low in comparison to numbers in non-depleted mice (Figure 7F), suggesting that the effects of anti-LTβR reflected effects on the stromal compartment and not on LTβR$^+$ CD11c$^+$ cells. Our results together suggest that the stromal disruption induced by DC depletion played an important role in disrupting the ongoing immune response and support the idea that a DC-stromal axis maintains immune responses.

DISCUSSION

Our data suggest a model whereby, upon the re-establishment of vascular-stromal quiescence, DCs maintain stromal integrity and, consequently, the ongoing immune response (Figure S7B). The localization of DCs in all compartments, the co-cultures of CD11c$^+$ cells and reticular cells, and the in vivo importance of DC-derived LTβR ligands, which are cell associated (Boulianne et al., 2012; Lu and Browning, 2014), support the idea that DCs act locally and directly to maintain reticular cell survival. The more numerous T and B cells also express LTβR ligands, suggesting scenarios that argue against DCs as direct mediators of reticular cell survival. One potential scenario is that DC depletion disrupted naive lymphocyte entry (Moussion and Girard, 2011) and that the resulting loss of lymphocyte-derived LTβR ligands primarily disrupted reticular cell survival. However, DC depletion during the re-establishment of quiescence activated endothelial cells and increased lymphocyte entry (data not shown). Additionally, DC depletion reduced lymphocyte numbers despite blockade of entry and exit, suggesting that lymphocyte loss was not primarily due to altered trafficking. Another possible scenario is that DCs act directly on lymphocytes to mediate lymphocyte survival and that the loss of lymphocyte-derived LTβR ligands upon DC depletion was the primary cause of reticular cell loss. Although DT treatment reduced lymph node cellularity of LTβ- and LIGHT-deficient but not WT mixed chimeras (data not shown), T and B cells do not express LTβR, suggesting that the loss of lymphocytes was secondary to reticular cell loss. The most conservative interpretation of our data, then, is that DCs directly maintain reticular cell survival and that the lymphocyte loss caused by disruption of the DC-stromal axis might amplify reticular cell loss. Resident DCs are relatively non-motile in comparison to lymphocytes (Bajénoff et al., 2006), and we speculate that prolonged association with reticular cells might allow more effective delivery of the membrane-bound signals.

Given the density of DCs in the T zone, a role for DCs in maintaining T zone function was less unexpected than the role in supporting follicular function. However, DCs were present in the follicles, and the high density within the mantle zone at the T-B boundary suggests the possibility that reticular cells in this region were among the CXCL13- and BAFF-expressing cells affected upon DC depletion. DCs more sparsely populated germinal centers, and these might directly maintain FDCs, which in turn might maintain germinal-center B cell survival, in part via BAFF. The fact that DC depletion reduced FDC numbers at a proportion similar to that of other reticular cell subsets suggests that germinal-center DCs are efficient regulators of FDC survival. Alternatively, disruption of the mantle zone with DC depletion might have also contributed to germinal-center disruption given that the reticular networks in these adjacent compartments are closely situated (Bannard et al., 2013). In follicles, then, our results suggested that DCs maintain total and germinal-center B cell survival at least in part by maintaining mantle-zone reticular cells and FDCs.

Our results implicate CD11c^{hi} DCs as key mediators of reticular cell survival during the re-establishment of quiescence: these DCs accumulated during this phase and were the most completely depleted in the zDC-DTR chimeras. This model whereby late-accumulating CD11c^{hi} DCs maintain PDPN expression and cell survival complements the recently proposed model whereby early-accumulating MHCII^{hi} DCs express CLEC-2 to inhibit PDPN-mediated cell contractility and allow lymph node growth (Acton et al., 2014; Astarita et al., 2015). However, our experiments do not rule out roles for other DC populations in mediating reticular cell survival, and further studies are needed if we are to understand the roles of each DC subset and the LTβR ligands each uses.

In addition to identifying a novel DC-LTβR-PDPN-reticular cell survival axis that supports immune responses, our findings highlight the idea that reticular cells at homeostasis and in immunized nodes are in different functional states. Reticular cell survival was regulated by DCs, PDPN, and cell adhesion only in stimulated nodes. This raises interesting questions about the drivers and other consequences of this functional change. These results also suggest that targeting a DC-stromal axis might allow specific targeting of inflamed lymph nodes in disease. Lymph nodes in a chronic lupus model appear to be in a state of re-established vascular, and presumably stromal, quiescence (Chyou et al., 2012), suggesting that a DC-stromal axis could maintain autoantibody generation. Such an axis might also exist in lymphoproliferative diseases and in tertiary lymphoid organs (Lambrecht and Hammad, 2012). Further understanding the role and regulation of the DC-stromal axis has the potential to lead to new therapeutic approaches for immune diseases.

EXPERIMENTAL PROCEDURES

Mice

Mice from 6–14 weeks old were used. C57Bl/6 mice were from The Jackson Laboratory (JAX), Taconic Farms, National Cancer Institute (NCI), or our own

breeding colony. Congenic CD45.1$^+$ mice were from NCI or our own breeding colony. *Cd11c*$^{-DTR}$ mice and *Rag1*$^{-/-}$ mice originally from JAX were bred at our facility and intercrossed to generate *Cd11c*$^{-DTR}$ *Rag1*$^{-/-}$ mice. zDC-DTR mice (Meredith et al., 2012) were bred at our facility. *Ltb*$^{-/-}$ mice (Koni et al., 1997) were intercrossed with *Rag1*$^{-/-}$ mice to generate *Ltb*$^{-/-}$ *Rag1*$^{-/-}$ mice in our facility. *Tnfsf14*$^{-/-}$ mice (Zhu et al., 2011) were intercrossed with *Rag1*$^{-/-}$ mice to generate *Tnfsf14*$^{-/-}$*Rag1*$^{-/-}$ mice at the University of Chicago. All animal procedures were performed in accordance with the regulations of the Institutional Animal Use and Care Committee at the Hospital for Special Surgery.

Flow-Cytometric Staining of Lymph Node Cells and Calculations

For flow-cytometric staining and analysis, lymph nodes were digested with type II collagenase (Worthington) prior to antibody staining (Chyou et al., 2011).

For calculations of cells per lymph node for the indicated cell populations, the percentage of the total gated population was multiplied by the total cell count per lymph node. For normalized values, the control sample was set to 1, and the value from the experimental sample was normalized accordingly. For experiments in which there was more than one control sample, the control values were averaged, and the individual control and experimental samples were calculated relative to this average value.

Enumeration of Germinal Centers in Tissue Sections

7 μm tissue sections were collected every five sections through the lymph node, and the largest (i.e., middle) five to ten sections were stained for IgD and either PNA (Vector) or both CD21 and CD35. Identifiable germinal centers (IgD$^-$ area that is either CD21$^+$ and CD35$^+$ or PNA$^+$) in each section were counted, and the maximal number of germinal centers per section was recorded.

Reticular Cell Cultures

PDPN$^+$ reticular cell cultures were generated as described (Benahmed et al., 2014). In brief, collagenase-digested lymph node cells were cultured for 7–8 days, depleted of CD45$^+$ and CD31$^+$ cells via magnetic selection, and used directly or passaged one time before use for experiments. SiRNA transfections were performed according to the manufacturer's instructions for the Oligofectamine Reagent kit (Invitrogen). For anti-LTbR experiments, at 48 hr after transfection, the media was changed to serum-free RPMI, and 3 μg/ml goat IgG or anti-LTβR (R&D Systems) was added. The cells were trypsinized 24 hr later and examined by flow cytometry. For Y27632 and anti-β1 experiments, cells were plated overnight to 80%–90% confluency, and treated with Y27632 at 10 μM (Acton et al., 2014; Astarita et al., 2015) (Calbiochem-EMD Millipore) or anti-β1 integrin (HMB1-1) at the indicated concentrations in serum-free media before being harvested at 48 hours for cell numbers and annexin V staining or at 24 hours for pFAK staining.

Cell-Adhesion Assay

For tests of cell adhesion, 96-well plates were coated with 20% FBS for 1 hr at 37°C. 5,000 reticular cells were added per well in serum-free media and allowed to adhere for 30 min before fixation and staining with 0.2% crystal violet in 2% ethanol for 20 min. Bound crystal violet was extracted with 50 μl 1% SDS, and OD was read at 590 nm.

SUPPLEMENTAL INFORMATION

Supplemental Information includes seven figures and Supplemental Experimental Procedures and can be found with this article online at http://dx.doi.org/10.1016/j.immuni.2015.03.015.

AUTHOR CONTRIBUTIONS

V.K., D.C.D., S.C., T.-C.T., C.R., and Y.L. designed, performed, and interpreted the experiments. Y.-X.F. and N.H.R. provided reagents and critical input on the manuscript. T.T.L. and W.S. designed and interpreted experiments. V.K. and T.T.L. wrote the paper.

ACKNOWLEDGMENTS

We acknowledge everyone in the Lu lab for helping hands, Alessandra Pernis and Jane Salmon and labs for helpful discussions, Michel Nussenzweig for zDC-DTR mice, and Jeff Browning and Adrian Erlebacher for helpful comments on the manuscript. This work was supported by R01 AI079178 (T.L.), the Alliance for Lupus Research (T.L.), and the St. Giles Foundation (T.L.).

Received: May 22, 2014
Revised: January 17, 2015
Accepted: February 28, 2015
Published: April 21, 2015

REFERENCES

Acton, S.E., Farrugia, A.J., Astarita, J.L., Mourão-Sá, D., Jenkins, R.P., Nye, E., Hooper, S., van Blijswijk, J., Rogers, N.C., Snelgrove, K.J., et al. (2014). Dendritic cells control fibroblastic reticular network tension and lymph node expansion. Nature *514*, 498–502.

Astarita, J.L., Acton, S.E., and Turley, S.J. (2012). Podoplanin: Emerging functions in development, the immune system, and cancer. Front. Immunol. *3*, 283.

Astarita, J.L., Cremasco, V., Fu, J., Darnell, M.C., Peck, J.R., Nieves-Bonilla, J.M., Song, K., Kondo, Y., Woodruff, M.C., Gogineni, A., et al. (2015). The CLEC-2-podoplanin axis controls the contractility of fibroblastic reticular cells and lymph node microarchitecture. Nat. Immunol. *16*, 75–84.

Bajénoff, M., Egen, J.G., Koo, L.Y., Laugier, J.P., Brau, F., Glaichenhaus, N., and Germain, R.N. (2006). Stromal cell networks regulate lymphocyte entry, migration, and territoriality in lymph nodes. Immunity *25*, 989–1001.

Bannard, O., Horton, R.M., Allen, C.D., An, J., Nagasawa, T., and Cyster, J.G. (2013). Germinal center centroblasts transition to a centrocyte phenotype according to a timed program and depend on the dark zone for effective selection. Immunity *39*, 912–924.

Baumjohann, D., Preite, S., Reboldi, A., Ronchi, F., Ansel, K.M., Lanzavecchia, A., and Sallusto, F. (2013). Persistent antigen and germinal center B cells sustain T follicular helper cell responses and phenotype. Immunity *38*, 596–605.

Benahmed, F., Chyou, S., Dasoveanu, D., Chen, J., Kumar, V., Iwakura, Y., and Lu, T.T. (2014). Multiple CD11c$^+$ cells collaboratively express IL-1β to modulate stromal vascular endothelial growth factor and lymph node vascular-stromal growth. J. Immunol. *192*, 4153–4163.

Boulianne, B., Porfilio, E.A., Pikor, N., and Gommerman, J.L. (2012). Lymphotoxin-sensitive microenvironments in homeostasis and inflammation. Front. Immunol. *3*, 243.

Braun, A., Worbs, T., Moschovakis, G.L., Halle, S., Hoffmann, K., Bölter, J., Münk, A., and Förster, R. (2011). Afferent lymph-derived T cells and DCs use different chemokine receptor CCR7-dependent routes for entry into the lymph node and intranodal migration. Nat. Immunol. *12*, 879–887.

Chyou, S., Benahmed, F., Chen, J., Kumar, V., Tian, S., Lipp, M., and Lu, T.T. (2011). Coordinated regulation of lymph node vascular-stromal growth first by CD11c$^+$ cells and then by T and B cells. J. Immunol. *187*, 5558–5567.

Chyou, S., Tian, S., Ekland, E.H., and Lu, T.T. (2012). Normalization of the lymph node T cell stromal microenvironment in lpr/lpr mice is associated with SU5416-induced reduction in autoantibodies. PLoS ONE *7*, e32828.

Cremasco, V., Woodruff, M.C., Onder, L., Cupovic, J., Nieves-Bonilla, J.M., Schildberg, F.A., Chang, J., Cremasco, F., Harvey, C.J., Wucherpfennig, K., et al. (2014). B cell homeostasis and follicle confines are governed by fibroblastic reticular cells. Nat. Immunol. *15*, 973–981.

Cyster, J.G. (2005). Chemokines, sphingosine-1-phosphate, and cell migration in secondary lymphoid organs. Annu. Rev. Immunol. *23*, 127–159.

Denton, A.E., Roberts, E.W., Linterman, M.A., and Fearon, D.T. (2014). Fibroblastic reticular cells of the lymph node are required for retention of resting but not activated CD8$^+$ T cells. Proc. Natl. Acad. Sci. USA *111*, 12139–12144.

Fornaro, M., Plescia, J., Chheang, S., Tallini, G., Zhu, Y.-M., King, M., Altieri, D.C., and Languino, L.R. (2003). Fibronectin protects prostate cancer cells from tumor necrosis factor-alpha-induced apoptosis via the AKT/survivin pathway. J. Biol. Chem. *278*, 50402–50411.

Geiger, B., Spatz, J.P., and Bershadsky, A.D. (2009). Environmental sensing through focal adhesions. Nat. Rev. Mol. Cell Biol. *10*, 21–33.

Hargreaves, D.C., Hyman, P.L., Lu, T.T., Ngo, V.N., Bidgol, A., Suzuki, G., Zou, Y.R., Littman, D.R., and Cyster, J.G. (2001). A coordinated change in chemokine responsiveness guides plasma cell movements. J. Exp. Med. *194*, 45–56.

Hase, H., Kanno, Y., Kojima, M., Hasegawa, K., Sakurai, D., Kojima, H., Tsuchiya, N., Tokunaga, K., Masawa, N., Azuma, M., et al. (2004). BAFF/BLyS can potentiate B-cell selection with the B-cell coreceptor complex. Blood *103*, 2257–2265.

Jarjour, M., Jorquera, A., Mondor, I., Wienert, S., Narang, P., Coles, M.C., Klauschen, F., and Bajénoff, M. (2014). Fate mapping reveals origin and dynamics of lymph node follicular dendritic cells. J. Exp. Med. *211*, 1109–1122.

Jung, S., Unutmaz, D., Wong, P., Sano, G., De los Santos, K., Sparwasser, T., Wu, S., Vuthoori, S., Ko, K., Zavala, F., et al. (2002). In vivo depletion of $CD11c^+$ dendritic cells abrogates priming of $CD8^+$ T cells by exogenous cell-associated antigens. Immunity *17*, 211–220.

Junt, T., Tumanov, A.V., Harris, N., Heikenwalder, M., Zeller, N., Kuprash, D.V., Aguzzi, A., Ludewig, B., Nedospasov, S.A., and Zinkernagel, R.M. (2006). Expression of lymphotoxin beta governs immunity at two distinct levels. Eur. J. Immunol. *36*, 2061–2075.

Katakai, T., Suto, H., Sugai, M., Gonda, H., Togawa, A., Suematsu, S., Ebisuno, Y., Katagiri, K., Kinashi, T., and Shimizu, A. (2008). Organizer-like reticular stromal cell layer common to adult secondary lymphoid organs. J. Immunol. *181*, 6189–6200.

Koni, P.A., Sacca, R., Lawton, P., Browning, J.L., Ruddle, N.H., and Flavell, R.A. (1997). Distinct roles in lymphoid organogenesis for lymphotoxins alpha and beta revealed in lymphotoxin beta-deficient mice. Immunity *6*, 491–500.

Lambrecht, B.N., and Hammad, H. (2012). Lung dendritic cells in respiratory viral infection and asthma: From protection to immunopathology. Annu. Rev. Immunol. *30*, 243–270.

Lesley, R., Xu, Y., Kalled, S.L., Hess, D.M., Schwab, S.R., Shu, H.B., and Cyster, J.G. (2004). Reduced competitiveness of autoantigen-engaged B cells due to increased dependence on BAFF. Immunity *20*, 441–453.

Link, A., Vogt, T.K., Favre, S., Britschgi, M.R., Acha-Orbea, H., Hinz, B., Cyster, J.G., and Luther, S.A. (2007). Fibroblastic reticular cells in lymph nodes regulate the homeostasis of naive T cells. Nat. Immunol. *8*, 1255–1265.

Lu, T.T., and Browning, J.L. (2014). Role of the lymphotoxin/LIGHT System in the development and maintenance of reticular networks and vasculature in lymphoid tissues. Front. Immunol. *5*, 47.

Mackay, F., and Leung, H. (2006). The role of the BAFF/APRIL system on T cell function. Semin. Immunol. *18*, 284–289.

Malhotra, D., Fletcher, A.L., and Turley, S.J. (2013). Stromal and hematopoietic cells in secondary lymphoid organs: partners in immunity. Immunol. Rev. *251*, 160–176.

Martín-Villar, E., Megías, D., Castel, S., Yurrita, M.M., Vilaró, S., and Quintanilla, M. (2006). Podoplanin binds ERM proteins to activate RhoA and promote epithelial-mesenchymal transition. J. Cell Sci. *119*, 4541–4553.

Merad, M., Sathe, P., Helft, J., Miller, J., and Mortha, A. (2013). The dendritic cell lineage: ontogeny and function of dendritic cells and their subsets in the steady state and the inflamed setting. Annu. Rev. Immunol. *31*, 563–604.

Meredith, M.M., Liu, K., Darrasse-Jeze, G., Kamphorst, A.O., Schreiber, H.A., Guermonprez, P., Idoyaga, J., Cheong, C., Yao, K.H., Niec, R.E., and Nussenzweig, M.C. (2012). Expression of the zinc finger transcription factor zDC (Zbtb46, Btbd4) defines the classical dendritic cell lineage. J. Exp. Med. *209*, 1153–1165.

Mionnet, C., Mondor, I., Jorquera, A., Loosveld, M., Maurizio, J., Arcangeli, M.L., Ruddle, N.H., Nowak, J., Aurrand-Lions, M., Luche, H., and Bajénoff, M. (2013). Identification of a new stromal cell type involved in the regulation of inflamed B cell follicles. PLoS Biol. *11*, e1001672.

Mitra, S.K., and Schlaepfer, D.D. (2006). Integrin-regulated FAK-Src signaling in normal and cancer cells. Curr. Opin. Cell Biol. *18*, 516–523.

Mohr, E., Serre, K., Manz, R.A., Cunningham, A.F., Khan, M., Hardie, D.L., Bird, R., and MacLennan, I.C.M. (2009). Dendritic cells and monocyte/macrophages that create the IL-6/APRIL-rich lymph node microenvironments where plasmablasts mature. J. Immunol. *182*, 2113–2123.

Moussion, C., and Girard, J.P. (2011). Dendritic cells control lymphocyte entry to lymph nodes through high endothelial venules. Nature *479*, 542–546.

Satpathy, A.T., Kc, W., Albring, J.C., Edelson, B.T., Kretzer, N.M., Bhattacharya, D., Murphy, T.L., and Murphy, K.M. (2012). Zbtb46 expression distinguishes classical dendritic cells and their committed progenitors from other immune lineages. J. Exp. Med. *209*, 1135–1152.

Schacht, V., Ramirez, M.I., Hong, Y.K., Hirakawa, S., Feng, D., Harvey, N., Williams, M., Dvorak, A.M., Dvorak, H.F., Oliver, G., and Detmar, M. (2003). T1alpha/podoplanin deficiency disrupts normal lymphatic vasculature formation and causes lymphedema. EMBO J. *22*, 3546–3556.

Suzuki, K., Maruya, M., Kawamoto, S., Sitnik, K., Kitamura, H., Agace, W.W., and Fagarasan, S. (2010). The sensing of environmental stimuli by follicular dendritic cells promotes immunoglobulin A generation in the gut. Immunity *33*, 71–83.

Tzeng, T.C., Chyou, S., Tian, S., Webster, B., Carpenter, A.C., Guaiquil, V.H., and Lu, T.T. (2010). CD11c(hi) dendritic cells regulate the re-establishment of vascular quiescence and stabilization after immune stimulation of lymph nodes. J. Immunol. *184*, 4247–4257.

Wang, X., Cho, B., Suzuki, K., Xu, Y., Green, J.A., An, J., and Cyster, J.G. (2011). Follicular dendritic cells help establish follicle identity and promote B cell retention in germinal centers. J. Exp. Med. *208*, 2497–2510.

Yang, C.-Y., Vogt, T.K., Favre, S., Scarpellino, L., Huang, H.-Y., Tacchini-Cottier, F., and Luther, S.A. (2014). Trapping of naive lymphocytes triggers rapid growth and remodeling of the fibroblast network in reactive murine lymph nodes. Proc. Natl. Acad. Sci. USA *111*, E109–E118.

Zhu, M., Yang, Y., Wang, Y., Wang, Z., and Fu, Y.-X. (2011). LIGHT regulates inflamed draining lymph node hypertrophy. J. Immunol. *186*, 7156–7163.

Immunity

Supplemental Information

A Dendritic-Cell-Stromal Axis Maintains Immune Responses in Lymph Nodes

Varsha Kumar, Dragos C. Dasoveanu Susan Chyou, Te-Chen Tzeng, Cristina Rozo, Yong Liang, William Stohl, Yang-Xin Fu, Nancy H. Ruddle, and Theresa T. Lu

Figure S1

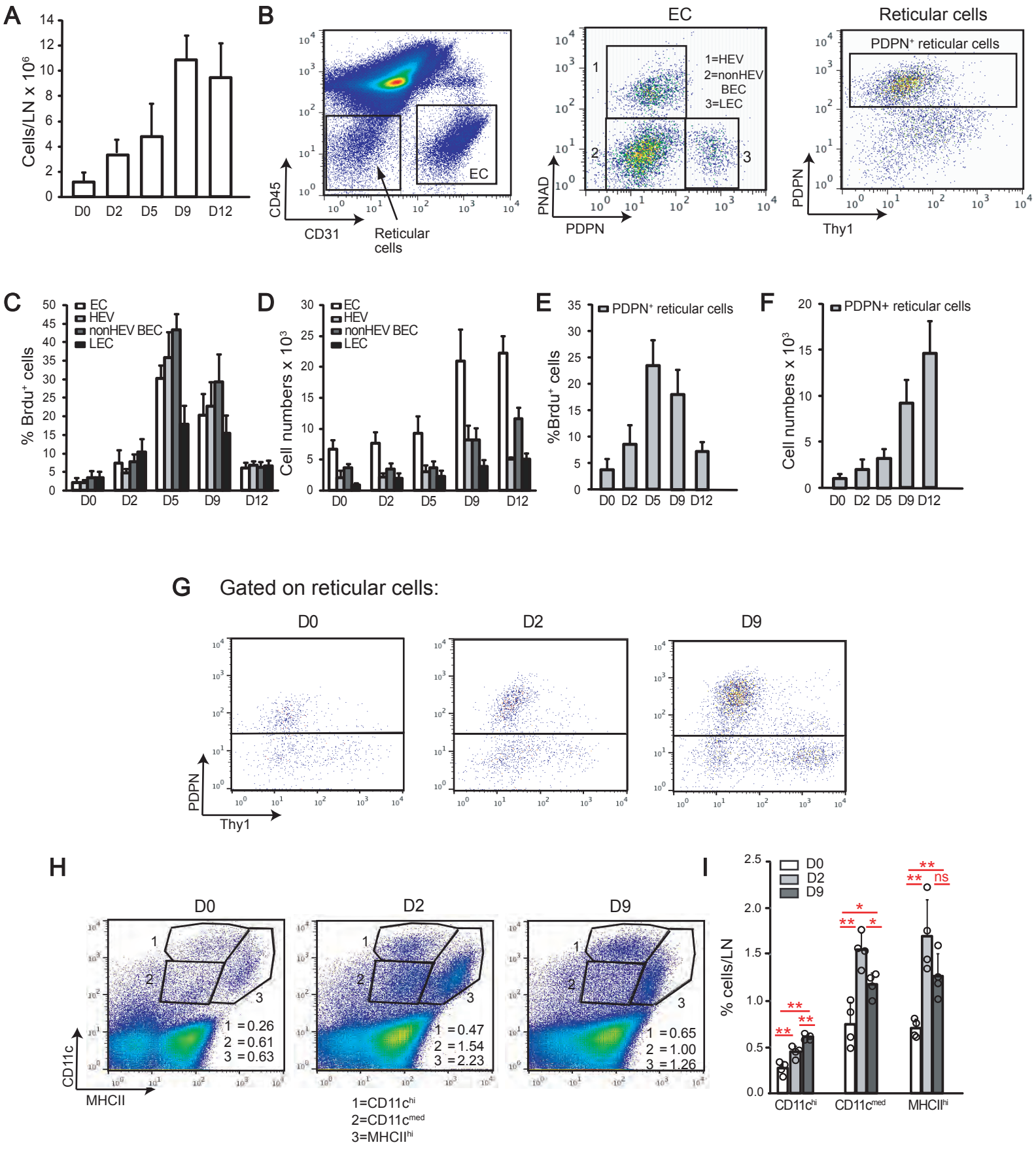
A
Cells/LN x 10^6
D0 D2 D5 D9 D12
B
CD45
CD31
EC
Reticular cells
EC
1=HEV
2=nonHEV BEC
3=LEC
PNAD
PDPN
Reticular cells
PDPN+ reticular cells
PDPN
Thy1
C
% Brdu+ cells
EC
HEV
nonHEV BEC
LEC
D0 D2 D5 D9 D12
D
Cell numbers x 10^3
EC
HEV
nonHEV BEC
LEC
D0 D2 D5 D9 D12
E
%Brdu+ cells
PDPN+ reticular cells
D0 D2 D5 D9 D12
F
Cell numbers x 10^3
PDPN+ reticular cells
D0 D2 D5 D9 D12
G
Gated on reticular cells:
D0
D2
D9
PDPN
Thy1
H
D0
D2
D9
1 = 0.26
2 = 0.61
3 = 0.63
1 = 0.47
2 = 1.54
3 = 2.23
1 = 0.65
2 = 1.00
3 = 1.26
CD11c
MHCII
1=CD11c^hi
2=CD11c^med
3=MHCII^hi
I
D0
D2
D9
% cells/LN
CD11c^hi
CD11c^med
MHCII^hi
**
*
ns

Figure S2

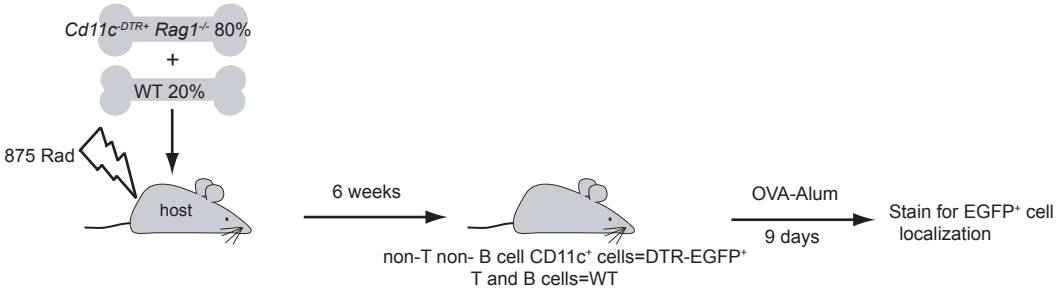
Cd11c-DTR+ Rag1-/- 80%
+
WT 20%
875 Rad
host
6 weeks
non-T non- B cell CD11c+ cells=DTR-EGFP+
T and B cells=WT
OVA-Alum
9 days
Stain for EGFP+ cell
localization

Figure S3

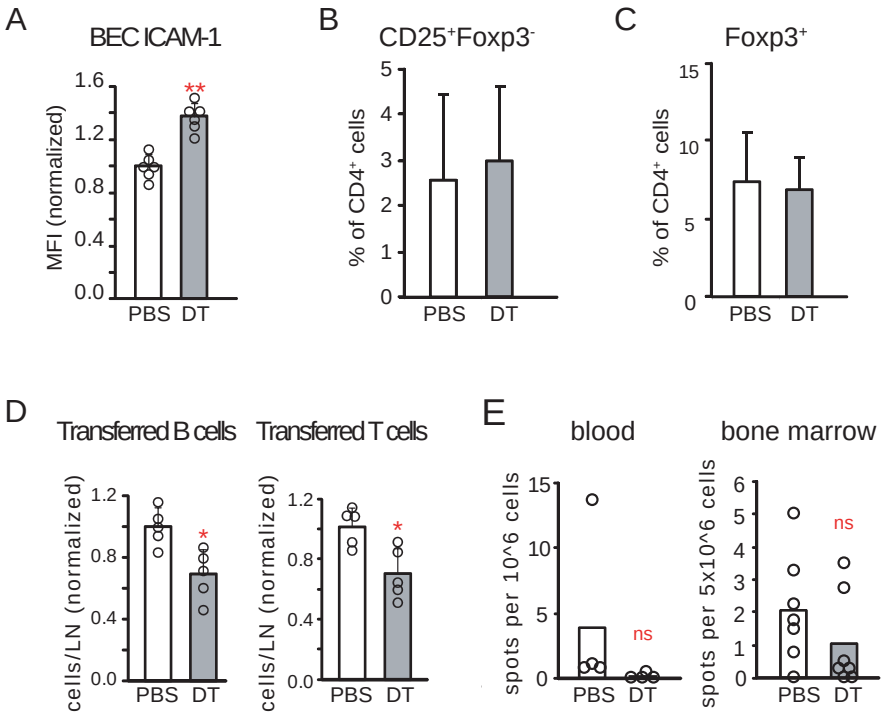
A
BEC ICAM-1
MFI (normalized)
1.6
1.2
0.8
0.4
0.0
**
PBS DT
B
CD25+Foxp3-
% of CD4+ cells
5
4
3
2
1
0
PBS DT
C
Foxp3+
% of CD4+ cells
15
10
5
0
PBS DT
D
Transferred B cells
cells/LN (normalized)
1.2
0.8
0.4
0.0
*
PBS DT
Transferred T cells
cells/LN (normalized)
1.2
0.8
0.4
0.0
*
PBS DT
E
blood
spots per 10^6 cells
15
10
5
0
ns
PBS DT
bone marrow
spots per 5x10^6 cells
6
5
4
3
2
1
0
ns
PBS DT

Figure S4

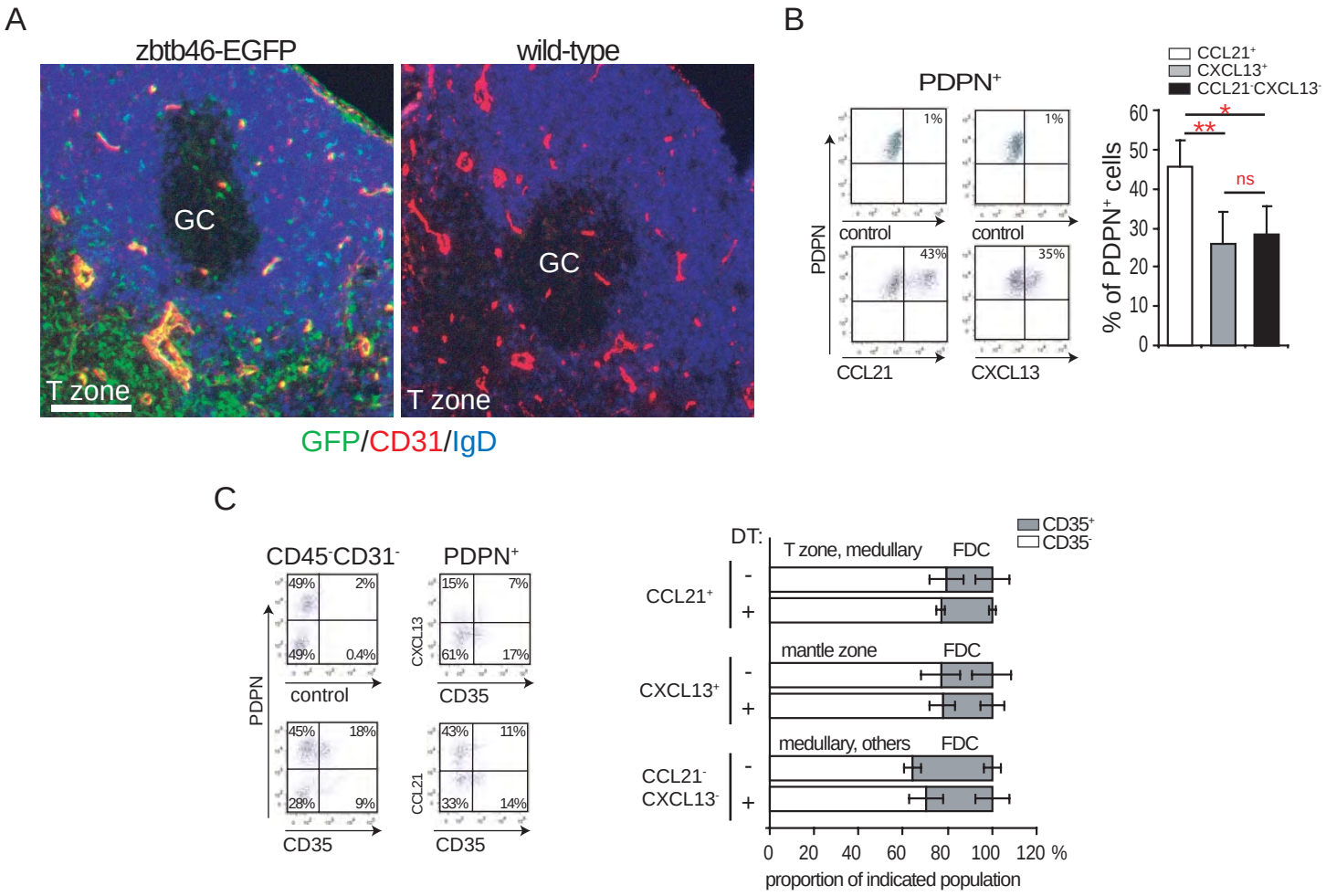
A
zbtb46-EGFP
wild-type
GC
GC
T zone
T zone
GFP/CD31/IgD
B
PDPN+
1%
1%
control
control
43%
35%
PDPN
CCL21
CXCL13
CCL21+
CXCL13+
CCL21-CXCL13-
% of PDPN+ cells
*
**
ns
C
CD45-CD31-
PDPN+
49%
2%
49%
0.4%
PDPN
control
15%
7%
61%
17%
CXCL13
CD35
45%
18%
28%
9%
CD35
43%
11%
33%
14%
CCL21
CD35
DT:
T zone, medullary
FDC
CCL21+
mantle zone
FDC
CXCL13+
medullary, others
FDC
CCL21-
CXCL13-
CD35+
CD35-
0 20 40 60 80 100 120 %
proportion of indicated population
D
PBS
DT
IgD/PNA
E
PBS
DT
IgD/activated caspase 3
F
PBS
DT
IgD/CD8
G
PDPN+
Lymph node
ns
ns
Cells/LN x 10^3
Cells/LN x 10^6
PBS
DT
PBS
DT

Figure S5

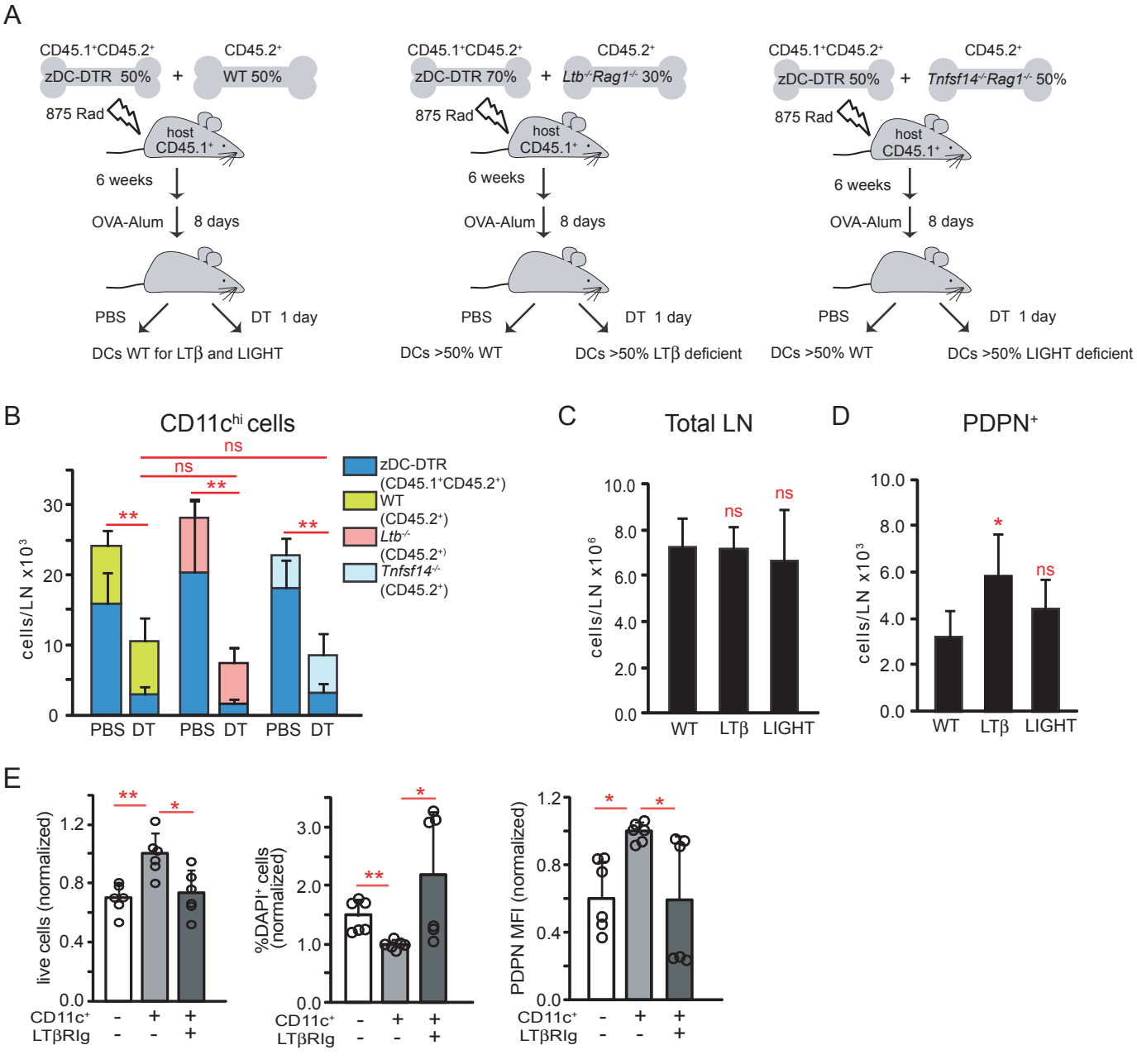
A
CD45.1+CD45.2+ zDC-DTR 50%
+
CD45.2+ WT 50%
875 Rad
host CD45.1+
6 weeks
OVA-Alum
8 days
PBS
DT 1 day
DCs WT for LTβ and LIGHT
CD45.1+CD45.2+ zDC-DTR 70%
+
CD45.2+ Ltb-/-Rag1-/- 30%
DCs >50% WT
DCs >50% LTβ deficient
CD45.1+CD45.2+ zDC-DTR 50%
+
CD45.2+ Tnfsf14-/-Rag1-/- 50%
DCs >50% WT
DCs >50% LIGHT deficient
B
CD11chi cells
cells/LN x10³
zDC-DTR (CD45.1+CD45.2+)
WT (CD45.2+)
Ltb-/- (CD45.2+)
Tnfsf14-/- (CD45.2+)
PBS DT PBS DT PBS DT
C
Total LN
cells/LN x10⁶
WT LTβ LIGHT
D
PDPN+
cells/LN x10³
WT LTβ LIGHT
E
live cells (normalized)
%DAPI+ cells (normalized)
PDPN MFI (normalized)
CD11c+
LTβRIg

Figure S6

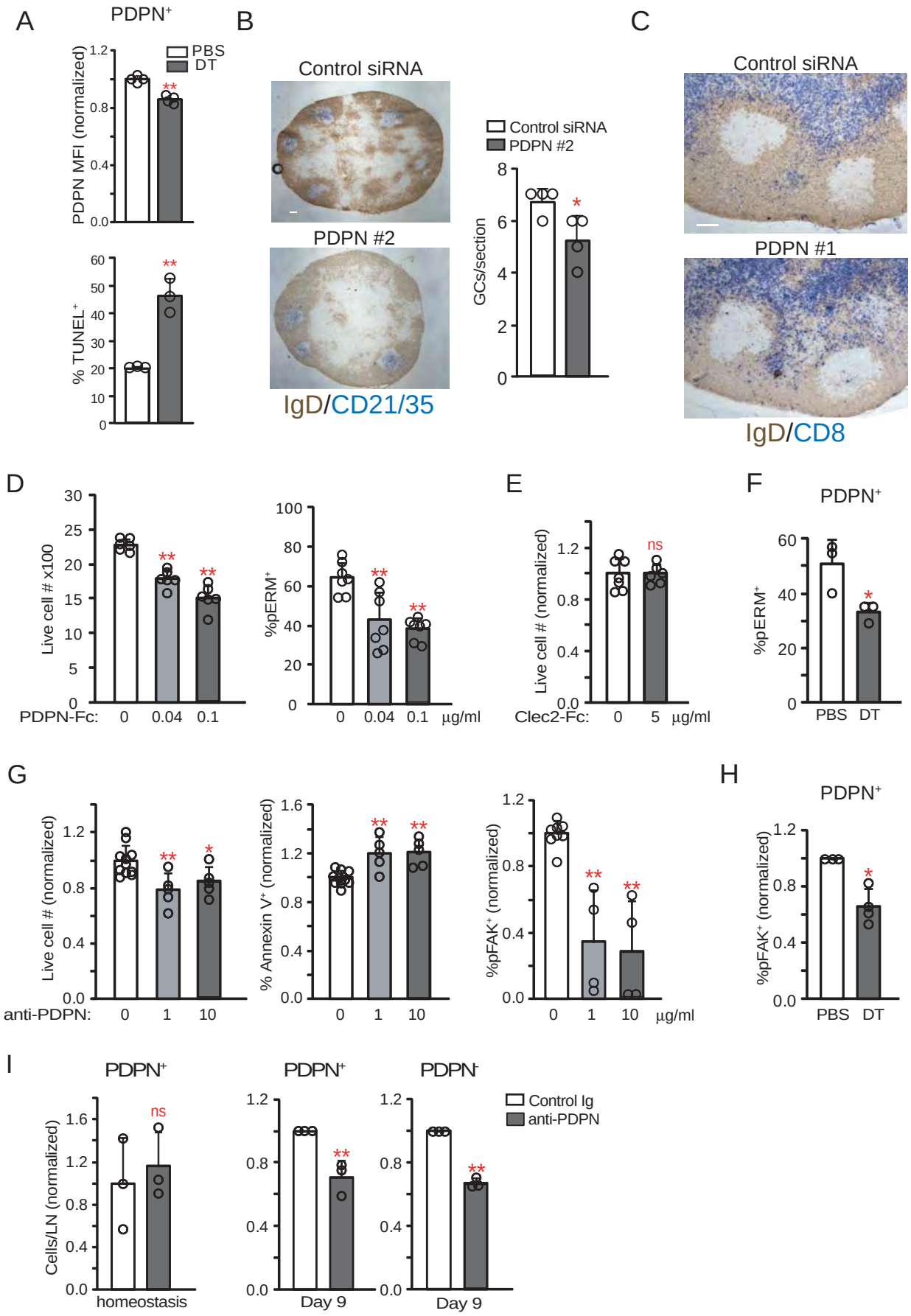
A
PDPN+
PBS
DT
PDPN MFI (normalized)
% TUNEL+
B
Control siRNA
PDPN #2
IgD/CD21/35
Control siRNA
PDPN #2
GCs/section
C
Control siRNA
PDPN #1
IgD/CD8
D
Live cell # x100
PDPN-Fc: 0 0.04 0.1
%pERM+
0 0.04 0.1 µg/ml
E
Live cell # (normalized)
ns
Clec2-Fc: 0 5 µg/ml
F
PDPN+
%pERM+
PBS DT
G
Live cell # (normalized)
anti-PDPN: 0 1 10
% Annexin V+ (normalized)
%pFAK+ (normalized)
0 1 10 µg/ml
H
PDPN+
%pFAK+ (normalized)
PBS DT
I
PDPN+
PDPN+
PDPN-
Cells/LN (normalized)
ns
homeostasis
Day 9
Day 9
Control Ig
anti-PDPN

Figure S7

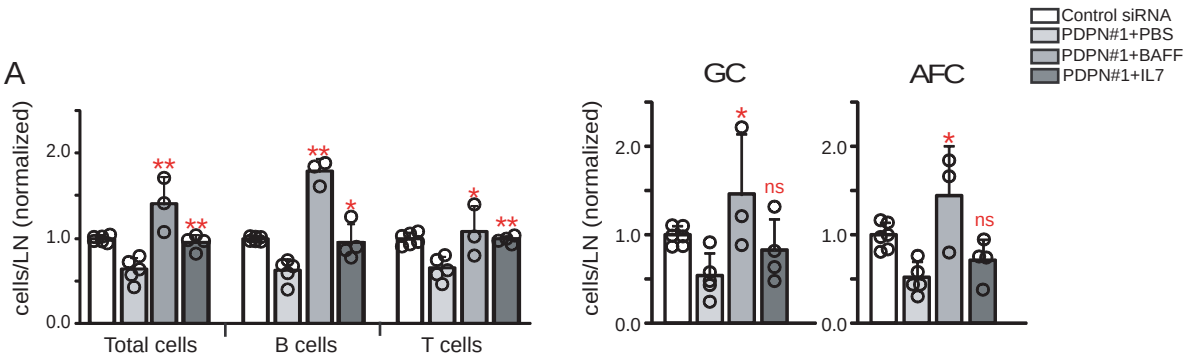
A
Control siRNA
PDPN#1+PBS
PDPN#1+BAFF
PDPN#1+IL7
cells/LN (normalized)
2.0
1.0
0.0
**
**
**
*
*
Total cells
B cells
T cells
GC
AFC
*
ns
*
ns

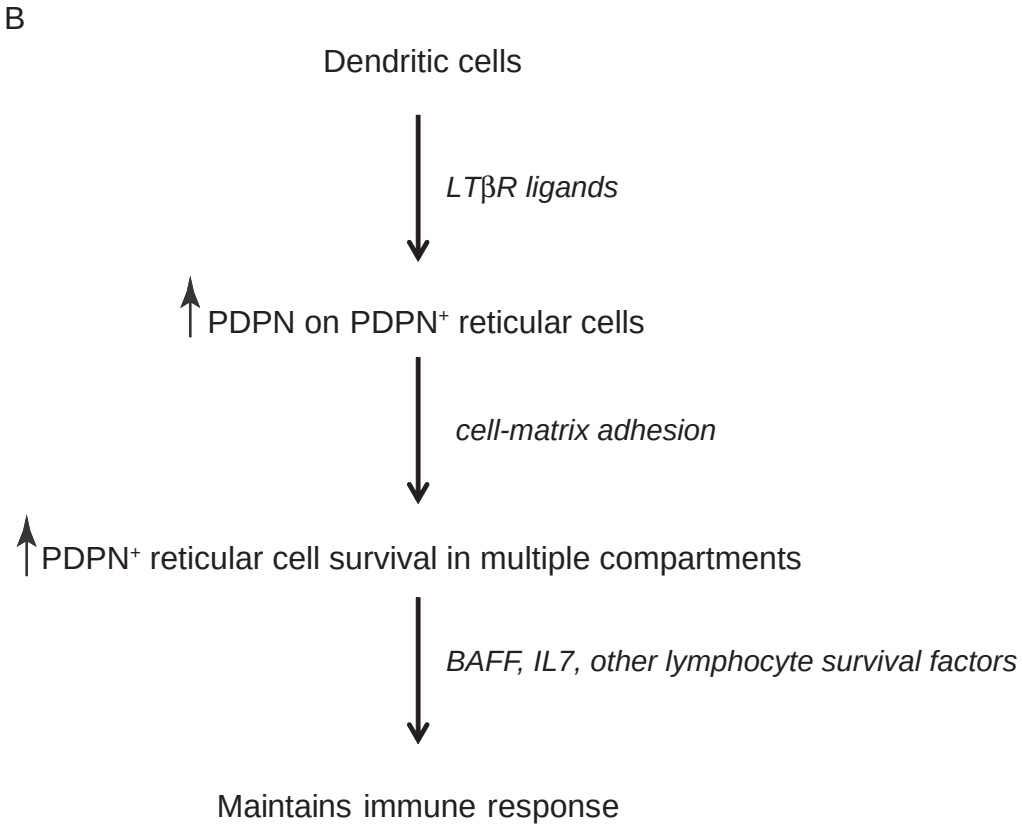
B
Dendritic cells
LTβR ligands
PDPN on PDPN+ reticular cells
cell-matrix adhesion
PDPN+ reticular cell survival in multiple compartments
BAFF, IL7, other lymphocyte survival factors
Maintains immune response

Supplemental Figure Legends

Figure S1. Characterization of vascular-stromal growth after OVA-Alum, related to Figure 1.

B6 mice were immunized in the footpads with OVA-Alum and draining popliteal lymph nodes were taken at indicated time points. Mice received 2mg bromodeoxyuridine (BrdU) injected IP at 24 hours and 1 hour prior to sacrifice and also received 0.8mg/ml BrDU in the drinking water between the injections. (A) Lymph node cellularity at the indicated time points. (B) FACS plots showing the gating for endothelial cell (EC) and reticular cell subsets. Endothelial cells are divided into $PNAd^+$ high endothelial venule (HEV), non-HEV blood endothelial cells (nonHEV BEC), and $PDPN^+$ lymphatic endothelial cells (LEC). Reticular cells can be divided into $PDPN^+$ and $PDPN^-$ subsets. (C) Proliferation rate of endothelial cell subsets as measured by the percentage of indicated cell subset that is $BrdU^+$. (D) Numbers of cells in each endothelial cell subset. (E) Proliferation rate of $PDPN^+$ reticular cells as measured by the percentage of cells that is $BrdU^+$. (F) Numbers of $PDPN^+$ reticular cells. For (A, C-F), $n \geq 6$ mice for each time point over 3 independent experiments. (G) FACS plots showing PDPN expression on reticular cells at indicated time points. Representative of at least 3 independent experiments. (H-I) Accumulation of $CD11c^+$ subsets over time. (H) Representative flow cytometry plots. (I) Pooled analysis of the percentage of each $CD11c^+$ subset over time. Each symbol represents 1 mouse; data from 2 independent experiments. Error bars represent SD. *=$p<.05$ and **=$p<.01$ by unpaired t-test.

Figure S2. Schematic of *Cd11c^{-DTR} Rag1$^{-/-}$* mixed chimeras, related to Figure 1.

Cd11c^{-DTR} Rag1$^{-/-}$ mixed chimeras were generated and immunized as outlined in the text. Chimerism of CD11c^{+} cells was 90% DTR^{+}:10% DTR^{-}, based on EGFP detection by flow cytometry (data not shown).

Figure S3. Effects of non-T non-B CD11c^{+} cell depletion, related to Figure 2.

Cd11c^{-DTR} Rag1$^{-/-}$ mixed chimeras were immunized in the footpads with OVA-Alum, treated with PBS or DT at day 8, and draining popliteal nodes were examined at day 9. (A) ICAM-1 MFI on (CD45^{-}CD31^{+}PDPN^{-}) blood endothelial cells. Each symbol represents a mouse. Data pooled from 4 experiments. (B-C) Percentage of CD4^{+} T cells that are (B) activated T cells (CD25^{+}Foxp3^{-}) or (C) regulatory T cells (Foxp3^{+}). n=8 mice per condition over 2 experiments. (D) Number of transferred lymphocytes upon CD11c^{+} cell depletion with simultaneous blockade of lymph node entry and egress. (CD45.2^{+}) CD11c-DTR mice received 2x10^{7} CD45.1^{+} splenocytes IV at day 7, 100ug anti-CD62L via retro-orbital injection and 50ug FTY720 IP at day 8, and four hours later, DT. CD45.1^{+} B220^{+} B cell and CD3^{+} T cell numbers in the draining popliteal lymph nodes were assessed on day 9. Data pooled from 3 independent experiments. (E) The number of anti-OVA AFCs in the blood and bone marrow, based on elispot assay. Data pooled from 3 experiments. For (A, D, E), each symbol represents 1 mouse. *=p<.05 and **=p<.01 by unpaired t-test.

Figure S4. DC localization and effects of DC depletion, related to Figure 3.

(A) Localization of zbtb46-expressing cells. *Zbtb46*-EGFP reporter mice were immunized in the footpads with OVA-Alum on day 0 and draining popliteal nodes were taken at day 9. Lymph nodes were fixed in 4% paraformaldehyde on ice for 1 hour and impregnated with 20% sucrose prior to freezing and subsequent sectioning and immunostaining. Cells that are $CD31^+$ and $EGFP^+$ are endothelial cells (Satpathy et al., 2012). Representative of 2 *Zbtb46*-EGFP mice. GC=germinal center. (B) Subsetting of $PDPN^+$ cells based on CCL21 and CXCL13 staining. Left: Flow cytometry plots showing CCL21 and CXCL13 staining of $PDPN^+$ reticular cells at day 9 after immunization. Right: Relative contributions of each subpopulation to the total $PDPN^+$ population. Bars represent n=5 mice over 3 experiments. (C) FDCs comprise a portion of each $PDPN^+$ subpopulation and $CD35^+$ and $CD35^-$ cells are proportionately lost with DC depletion. Left: Flow cytometry plots showing CD35 staining on $CD45^-CD31^-$ reticular cells and CXCL13 and CCL21 staining in $PDPN^+CD35^+$ FDCs at day 9. Right: Relative contributions of $CD35^+$ and $CD35^-$ cells to $PDPN^+$ subpopulations in day 9 zDC-DTR chimeras treated for 24 hours with PBS or DT. For $CD35^+CCL21^-CXL13^-$ cells, $CD35^+CCL21^+$ and $CD35^+CXL13^+$ were subtracted from total $PDPN^+CD35^+$ numbers, and this number was expressed as a proportion of $PDPN^+CCL21^-CXL13^-$ cells. Bars represent 3 mice per condition over 2 experiments. (D-F) Immunostained sections of day 9 zDC-DTR chimeras treated for 24 hours with PBS or DT. (D) Gross follicular morphology. (E) Activated caspase 3 in germinal centers. (F) Compartmental integrity, in a different pair of mice from that shown in Figure 3I. (D-F), representative of 3 pairs of mice from 3 experiments. (G) $PDPN^+$ reticular cell numbers and lymph node cellularity upon DC depletion at homeostasis. Homeostatic zDC-DTR chimeras were

treated with PBS or DT and popliteal and paraaortic nodes were pooled and examined the next day. n=4 mice per condition over 2 experiments. Bars represent SD. (A, D, E, F) White bar=100um. *=p<.05, **=p<.01, and ns=not significant by unpaired t-test.

Figure S5. Role of DC-derived LTβR ligands, related to Figure 5.

(A) Schematic of zDC-DTR:WT or LTβ or LIGHT-deficient mixed chimeras. $CD45.1^+$ recipients were given a 50:50 mix of $CD45.1^+CD45.2^+$ zDC-DTR and $CD45.2^+$ WT or *Tnfsf14*$^{-/-}$*Rag1*$^{-/-}$ bone marrow. For zDC-DTR:LTβ chimeras, a 70:30 mix of $CD45.1^+CD45.2^+$ zDC-DTR and $CD45.2^+$ *Ltb*$^{-/-}$*Rag1*$^{-/-}$ bone marrow was used, based on unpublished preliminary observations of relative reconstitution rates. After reconstitution, the chimeras were immunized in the footpads with OVA-Alum, treated with PBS or DT at day 8, and draining popliteal nodes were taken at day 9. (B-D) Analysis of the mixed chimeras depicted in (A). (B) $CD11c^{hi}$ cell numbers in PBS and DT-treated chimeras. Contributions of the different donors are shown. (C) Lymph node cellularity in PBS-treated chimeras. (D) $PDPN^+$ reticular cell numbers in PBS-treated chimeras. (B-D) n=3-8 mice per condition over 3 experiments for each of the LTβ and LIGHT-deficient chimeras. (E) Effect of $CD11c^+$ cells on reticular cells in vitro. $CD11c^+$ cells from day 9 lymph nodes were sorted by flow cytometry and added at 100,000 cells per well to confluent reticular cells in 96-well plates. At 24 hours after $CD11c^+$ cell addition, media was changed to serum-free RPMI and LTβR-Ig or control Ig was added at 10ug/ml. Cultures were harvested and counted by flow cytometry 2 days later. Left: Number of $CD45^-DAPI^-$ reticular cells. Middle: Percent of all $CD45^-$ cells that are $DAPI^+$. Right: Geometric mean fluorescence intensity of PDPN on $CD45^-DAPI^-$

reticular cells. Each symbol represents one well, and numbers are normalized relative to numbers in the "+ $CD11c^+$ cells" condition (middle bar). Data are pooled from 2 experiments with 3 wells per condition per experiment. Results are representative of 4 similar experiments. For (B-E), *=p<.05 and **=p<.01 by unpaired t-test.

Figure S6. PDPN regulation and effects of PDPN knockdown or blockade, related to Figure 6.

(A) Early $PDPN^+$ reticular cell alterations upon DC depletion. PDPN geometric mean fluorescence intensity and TUNEL staining were examined at 5.5-8 hours after DT treatment of zDC-DTR chimeras on day 8. Data pooled from 3 experiments. (B) Germinal center numbers with PDPN-targeted siRNA. Left: Sections stained for IgD and CD21/CD35. Right: Number of germinal centers per tissue section. Pooled analysis of 4 pairs of mice. (C) Compartmental integrity with PDPN-targeted siRNA. Representative of at least 3 pairs of mice. (D-E) $PDPN^+$ reticular cells were plated to 80-90% confluency overnight, and then treated with indicated reagents in serum-free media and examined by flow cytometry 24-48 hours later. (D) PDPN-Fc at indicated concentrations (Acton et al., 2012). Cells were analyzed at 24 hours for pERM and 48 hours for $DAPI^-$ cell numbers. Data pooled from 2 experiments for each time point, with at least 3 wells per condition per experiment. (E) CLEC-2-Fc at indicated concentrations (Astarita et al., 2015). $DAPI^-$ cell numbers were analyzed at 48 hours. Data pooled from 2 experiments with 3-4 wells per condition per experiment. (F) pERM expression in $PDPN^+$ reticular cells in zDC-DTR chimeras at 5.5-8 hours after DT injection on day 8. Data pooled from 3 experiments. (G) Effects of anti-PDPN at indicated concentrations (Astarita et al.,

2015) on DAPI$^-$ cell counts and Annexin V binding at 48 hours and pFAK expression at 24 hours. Cells were treated as in (D-E). Data pooled from 2 experiments per time point, with 2-7 wells per condition per experiment. (H) pFAK expression in PDPN$^+$ reticular cells in zDC-DTR chimeras at 5.5-8 hours after DT injection on day 8. Data pooled from 3 experiments. (I) PDPN$^+$ reticular cell numbers in homeostatic and day 9 mice given 100ug control IgG or anti-PDPN via retroorbital injection at 24 hours before sacrifice. Each symbol represents 1 mouse and results are pooled from 2 (homeostasis) or 3 (immunized) independent experiments. For (A-I), *=p<.05, **=p<.01, and ns=not significant by t-test when compared to control.

Figure S7. Survival factor administration upon PDPN knockdown and model of the DC-stromal axis, related to Figure 7.

(A) BAFF and IL-7 replacement with PDPN knockdown. Mice were given either control or PDPN#1 siRNA on days 6 and 7. Indicated PDPN#1-treated mice were given BAFF or IL-7 on day 8 and examined on day 9. The numbers of cells in indicated populations were normalized and compared to PDPN#1+PBS numbers. Each symbol represents 1 mouse; data pooled from 3 experiments. (B) Model of the DC-stromal axis.

Supplemental Experimental Procedures

Mice:

Zbtb46-EGFP mice (Satpathy et al., 2012) were purchased from the Jackson Laboratory and bred at our facility. *Zbtb46*-EGFP$^{+/-}$ mice were used for experiments.

Mouse immunization and treatments:

Unless otherwise specified, mice were immunized with OVA in Alum (OVA-Alum) by hind footpad injection of 20 µl of 1mg/ml OVA-Alum. For flow cytometry sorting of stromal cells and CD11c^{+} cells, mice were administered 20ul OVA-Alum in hind footpads and 50ul at tail base, and draining popliteal, inguinal, and periaortic nodes were taken. For *Cd11c*$^{-DTR}$ *Rag1*$^{-/-}$ chimera experiments, 200ug of DT was given IP. For zDC-DTR chimeras, 20ng DT per gram body weight was given IP. For LTβR-Ig experiments, mice were injected retroorbitally with 100ug of mLTβR-mIgG1 (Biogen Idec, Cambridge, MA) or control mouse IgG1 clone MOPC21 (Biogen Idec, Cambridge, MA). For siRNA experiments, 50ug of siRNA (Thermo Scientific, Waltham, MA) per dose in 500ul of PBS was injected via tail vein. SiRNA#1 sequence was 5'-GCUGCAUCUUUCUGGAUAATT-3' and siRNA#2 was 5'-CGCAGACAACAGAUAAGAATT-3'(Acton et al., 2012). Control siRNA was from Qiagen (All Stars Negative Control). For anti-β1 integrin treatments, 20ug of anti- β1 (clone HMB1-1, Biolegend, San Diego, CA) (Ridger et al., 2001) was injected via tail vein. For BAFF and IL-7 replacement experiments, PBS, 10ug recombinant hBAFF (Peprotech, Rocky Hill, NJ), or 1.5ug mIL-7 (Peprotech) was injected via tail vein. For anti-LTβR treatment of zDC-DTR chimeras, 20ug of polyclonal anti-LTβR (as used in

(Katakai et al., 2004)) or goat IgG control (both from R&D Systems, Minneapolis, MN) was injected retroorbitally.

For bone marrow chimeras, recipients were lethally irradiated using one dose of 875 rads from an X-ray source as previously described (Chyou et al., 2011) and then reconstituted for at least 6 weeks.

Flow cytometric staining and sorting:

Antibodies for extracellular markers were against CD45 (BD Biosciences, San Jose, CA), CD31 (BD Biosciences), PDPN (BioLegend, San Diego, CA, or Developmental Studies Hybridoma Bank, Iowa City, IA), Thy1 (BD Biosciences), MHCII (BioLegend), CD11c (BD Biosciences), B220 (Biolegend), CD3 (Biolegend), CD35 (Clone 8C12, BD Biosciences), CD16/CD32 (Fc block; BD Biosciences). PNA was from Vector Laboratories, Burlingame, CA). As CD138 staining was not detectable in collagenase-digested samples, AFCs were detected by intracellular staining with anti-mouse IgG (BD Biosciences), performed using the BD Cytofix/Cytoperm kit. Cells were analyzed using a FACSCanto (BD Biosciences) and FlowJo software (Tree Star, Ashland, OR).

For intracellular staining of chemokines, cells were fixed and permeabilized with BD Cytofix/Cytoperm after extracellular marker staining. Cells were incubated with additional Fc block x 10 minutes and then anti-CXCL13 (AF470), anti-CCL21 (AF457), or control goat IgG (all R&D Systems) for 40 minutes on ice. Primary antibodies were detected with anti-goat Alexa Fluor-647 (Jackson ImmunoResearch).

TUNEL staining was performed essentially according to manufacturer's instructions (Roche, Indianapolis, IN). Briefly, after extracellular marker staining, cells were fixed in 2% paraformaldehyde at room temperature for 30 minutes followed by permeabilization with 0.1% TritonX-100 in 0.1% sodium citrate for 2 minutes on ice. The cells were washed twice with PBS, incubated with terminal deoxynucleotidyl transferase and fluorescein-dUTP at 37 degrees Celsius for one hour, followed by two washes in PBS. Fluorescence was detected by flow cytometry.

For staining of pERM or pFAK (Belkina et al., 2009; Han et al., 2011), lymph nodes cells after enzymatic digestion were immediately fixed in 1% paraformaldehyde for 20 minutes on ice followed by extracellular marker staining. The cells were then treated with eBioscience fixation/permeabilization buffer for 30 minutes at room temperature with periodic pipetting to avoid clumping. The cells were incubated with Fc block for 10 minutes and then with antibody against pERM (Ab 3141, Cell Signaling Technology, Danvers, MA) or pFAK at Y397 (ABT135, Millipore, Billerica, MA) or control rabbit antibody (BD Biosciences) for 40 minutes at room temperature. Primary antibodies were detected with anti-rabbit Alexa-Fluor 647 (Jackson ImmunoResearch). For staining of pERM or pFAK in cultured reticular cells, cells were trypsinized (0.25% Trypsin/EDTA, Life Technology, Grand Island, NY) followed by extracellular marker staining. Cells were treated with fixation/permeabilization buffer on ice for pERM and on ice or at room temperature for pFAK for 30 minutes. Cell were then treated with Fc block for 10

minutes and stained with anti- pERM, anti-pFAK or control Ig for 40 minutes on ice. Primary antibodies were detected with anti-rabbit Alexa-Fluor 488 (Life Technology).

Annexin V staining of cultured reticular cells was performed per manufacturer's instructions (BD Biosciences).

For flow cytometric sorting of reticular cells, lymph nodes were digested with collagenase and then subject to CD45 depletion by magnetic selection (Miltenyi, Cambridge, MA) prior to sorting. For sorting of $CD11c^+$ cell subsets, digested lymph node cells were depleted of IgD^+ and $CD3^+$ cells prior to sorting. Cells were sorted using a BD FACSVantage. Purity of sorted populations were $\geq$95%.

Real time PCR:

Cells were lysed and RNA extracted using the RNeasy Minikit (Qiagen, Venlo, Netherlands). iScript cDNA synthesis kit (Bio-Rad, Hercules, CA) was used to generate cDNA. IQ Sybr-Green Supermix kit (Bio-Rad, Hercules, CA) was used for real-time PCR. Gene expression was quantitated relative to GAPDH expression.

The following primers were used:

BAFF F: 5'- -3	TGCCTTGGAGGAGAAAGAGA
BAFF R: 5'- -3'	GGAATTGTTGGGCAGTGTTT
IL-6 F: 5'- -3	GCCAGAGTCCTTCAGAGAG
IL-6 R: 5'- -3'	ACTCCTTCTGTGACTCCAGC
IL-7 F: 5'- -3	CTGAAAGTGATAAGGGTTTG

IL-7 R: 5'- -3'	CTGAGTAGAGCATTATAGGG
LTα F: 5'- -3	GCTTGGCACCCCTCCTGTC
LTα R: 5'- -3'	GATGCCATGGGTCAAGTGCT
LTβ F: 5'- -3'	CCAGCTGCGGATTCTACACCA
LTβ R: 5'- -3'	AGCCCTTGCCCACTCATCC
LIGHT F: 5'- -3'	CCTGAGACTGCATCAACGTC
LIGHT R: 5'- -3'	TTGGCTCCTGTAAGATGTGC
GAPDH F: 5'- -3'	ATGTGTCCGTCGTGGATCTGA
GAPDH R: 5'- -3'	TTGAAGTCGCAGGAGACAACCT

Staining of lymph node sections:

Procedure is as previously described (Webster et al., 2006). Tissues were frozen fresh in OCT. Seven um sections were cut and fixed in cold acetone for 10 minutes before applying primary antibody. Primary antibodies used were against ER-TR7 (Biolegend), desmin (Thermo Scientific), PDPN (Developmental Studies Hybridoma Bank, Iowa City, IA), IgD (eBioscience), CD21/CD35 (clone 7E9, Biolegend), CD3 (BD Biosciences), rabbit-anti-EGFP (Invitrogen, Carlsbad, CA), CD8 (Biolegend). For immunohistochemistry, secondary antibodies or streptavidin were conjugated to alkaline-phosphatase or horseradish peroxidase and visualized using Naphthol AS-MX phosphate with Fast Blue or Fast Red salt (Sigma-Aldrich, St. Louis, MO) or diaminobenzidine (Pierce Chemical Co., Rockford, IL). For immunofluorescence, primary antibodies were detected with anti-rat-Alexa Fluor 488 (Invitrogen), anti-rabbit-rhodamine (Jackson ImmunoResearch, West Grove, PA), streptavidin-AMCA (Jackson ImmunoResearch).

Elispot assay:

Procedure is essentially as described (Hargreaves et al., 2001). Wells were coated with 0.1% ovalbumin and cells isolated from peripheral blood and bone marrow ($1x10^6$ for blood and $20x10^6$ for bone marrow) were added and incubated at 37°C for 4 hours. Anti-mouse IgG-biotin was applied, followed by streptavidin-conjugated alkaline phosphatase, and spots were visualized using 5-bromo-4-chloro-3-indolyl phosphate (Sigma-Aldrich).

Additional reagents:

PDPN-Fc and control rabbit IgG were from R&D Systems. Anti-PDPN (clone 8.1.1) and control hamster IgG were purchased in low endotoxin/azide-free format from Biolegend for in vivo and in vitro experiments. For immunostaining, anti-GFP-AlexaFluor 488 (Invitrogen), anti-active caspase 3 (R&D Systems), CD31 (clone 2H8, gift of William Muller), anti-armenian hamster rhodamine (Jackson Immunoresearch), and anti-rat-AlexaFluor350 (Invitrogen) were additionally used. Anti-CD62L was from BD Biosciences and FTY720 was from Calbiochem (Darmstadt, Germany).

Supplemental References

Acton, S. E., Astarita, J. L., Malhotra, D., Lukacs-Kornek, V., Franz, B., Hess, P. R., Jakus, Z., Kuligowski, M., Fletcher, A. L., Elpek, K. G., *et al.* (2012). Podoplanin-rich stromal networks induce dendritic cell motility via activation of the C-type lectin receptor CLEC-2. Immunity *37*, 276-289.

Belkina, N. V., Liu, Y., Hao, J. J., Karasuyama, H., and Shaw, S. (2009). LOK is a major ERM kinase in resting lymphocytes and regulates cytoskeletal rearrangement through ERM phosphorylation. Proc Natl Acad Sci U S A *106*, 4707-4712.

Han, B., Qi, S., Hu, B., Luo, H., and Wu, J. (2011). TGF-beta i promotes islet beta-cell function and regeneration. J Immunol *186*, 5833-5844.

Katakai, T., Hara, T., Sugai, M., Gonda, H., and Shimizu, A. (2004). Lymph node fibroblastic reticular cells construct the stromal reticulum via contact with lymphocytes. J Exp Med *200*, 783-795.

Ridger, V. C., Wagner, B. E., Wallace, W. A. H., and Hellewell, P. G. (2001). Differential effects of CD18, CD29, and CD49 integrin subunit inhibition on neutrophil migration in pulmonary inflammation. J Immunol *166*, 3484-3490.

Webster, B., Ekland, E. H., Agle, L. M., Chyou, S., Ruggieri, R., and Lu, T. T. (2006). Regulation of lymph node vascular growth by dendritic cells. J Exp Med *203*, 1903-1913.